Masui T.	Trust and Creation of Biobanks: biobanking in Japan and the UK.	M. Sleeboom-Falker, ed. Biobanking.			. 2007 in press
増井徹.	包括同意、何が問題か：医学・生物学研究をめぐる内外の状況から.	メディカルバイオエシックス2007	34	74-81.	
Masui T, Liu SY, Tamaoki E, Tsutani K.	Ethics in phamacogenetics: Harms caused by genetic exceptionalism.	Pharmacogenetics			2007 in revision
増井徹　ほか.	医療・医薬品バイオ技術に関する国民理解促進施策研究会提言；医療・医薬品に関わるバイオ技術の円滑な産業化を目指す情報発信について、	関西経済連合会、産業・科学技術委員会	2006	1-20	
Harasawa R, Aoyama F, Goryo M, Okada K, Nishimura T, Matsubara K, Tsujimoto T, Giangaspero M.	Evidence for pestivirus infection in free-living Japanese serows, Capricornis crispus.	Microbiol Immunol	50(10)	817-21	2006
Harasawa R, Tanabe H, Kurematsu M, Mizusawa H, Suzuki Y.	Self-propagating calciferous particles detected in a human cell line Kasumi-6 (JCRB1024).	In Vitro Cell Dev Biol Anim.	42(1-2)	13-5	2006
Giangaspero M, Harasawa R, Muschko K, Büttner M.	Characteristics of the 5' untranslated region of wisent (Bison bonasus) and reindeer (Rangifer tarandus) Pestivirus isolates.	Veterinaria Italiana	42(3)	165-172	2006

Similarities and Differences between Cyclobutane Pyrimidine Dimer Photolyase and (6-4) Photolyase as Revealed by Resonance Raman Spectroscopy

ELECTRON TRANSFER FROM THE FAD COFACTOR TO ULTRAVIOLET-DAMAGED DNA*

Jiang Li[‡§1], Takeshi Uchida[‡§2], Takeshi Todo[¶], and Teizo Kitagawa[‡§3]

From the ‡Okazaki Institute for Integrative Bioscience, National Institutes of Natural Sciences, Myodaiji, Okazaki, Aichi 444-8787, the §Department of Photoscience, School of Advanced Sciences, Graduate University for Advanced Studies, Shonan Village, Hayama, Kanagawa 240-0193, and the ¶Radiation Biology Center, Kyoto University, Yoshidakonoe-cho, Sakyo-ku, Kyoto 606-8501, Japan

The cyclobutane pyrimidine dimer (CPD) and (6-4) photoproduct, two major types of DNA damage caused by UV light, are repaired under illumination with near UV-visible light by CPD and (6-4) photolyases, respectively. To understand the mechanism of DNA repair, we examined the resonance Raman spectra of complexes between damaged DNA and the neutral semiquinoid and oxidized forms of (6-4) and CPD photolyases. The marker band for a neutral semiquinoid flavin and band I of the oxidized flavin, which are derived from the vibrations of the benzene ring of FAD, were shifted to lower frequencies upon binding of damaged DNA by CPD photolyase but not by (6-4) photolyase, indicating that CPD interacts with the benzene ring of FAD directly but that the (6-4) photoproduct does not. Bands II and VII of the oxidized flavin and the 1398/1391 cm^{-1} bands of the neutral semiquinoid flavin, which may reflect the bending of U-shaped FAD, were altered upon substrate binding, suggesting that CPD and the (6-4) photoproduct interact with the adenine ring of FAD. When substrate was bound, there was an upshifted 1528 cm^{-1} band of the neutral semiquinoid flavin in CPD photolyase, indicating a weakened hydrogen bond at N(5)–H of FAD, and band X seemed to be downshifted in (6-4) photolyase, indicating a weakened hydrogen bond at N(3)–H of FAD. These Raman spectra led us to conclude that the two photolyases have different electron transfer mechanisms as well as different hydrogen bonding environments, which account for the higher redox potential of CPD photolyase.

Irradiation of organisms with ultraviolet light causes damage to cellular DNA by inducing dimer formation between adjacent pyrimidine bases. This DNA damage causes mutation and cell death and can lead to cancer (1). The cyclobutane pyrimidine dimer (CPD)[4] and (6-4) photoproduct (Fig. 1) account for most of this DNA damage, and these are repaired by CPD and (6-4) photolyases, respectively, under illumination by near UV-visible light (2, 3). Similar association constants of $\sim 10^{-9}$ M were identified for CPD and the (6-4) photoproduct in the complex of the corresponding photolyase, respectively, whereas those for the undamaged DNA were >4 orders of magnitude lower or not detectable (4–6). Both photolyases contain FAD as an essential catalytic cofactor (7, 8). The amino acid sequences of (6-4) and CPD photolyases, especially within the FAD-binding region, are closely related, suggesting that these two enzymes share similar structure and reaction mechanisms (9); however, the quantum yield for photorecovery is significantly lower for (6-4) photolyase than for CPD photolyase (4, 6, 10).

The isoalloxazine ring of FAD in a photolyase can exist in one of three possible states: oxidized (FAD_{ox}), neutral semiquinoid (FADH°), and anionic fully reduced ($FADH^-$) forms (Fig. 2). $FADH^-$ is considered to be the active form of flavin in photolyase. The first step of the repair process is the specific recognition of CPD and the (6-4) photoproduct by CPD photolyase (2) and (6-4) photolyase (9), respectively. After photoexcitation of $FADH^-$ by near UV-visible light, an electron is transferred to the damaged DNA, leaving the flavin in the neutral semiquinoid form (FADH°). Following bond cleavage of the DNA dimer, the electron is transferred back to FADH° to restore the active state, $FADH^-$ (4). In the case of the (6-4) photoproduct, it has been proposed that the bound substrate is converted to a four-membered oxetane ring intermediate (10) catalyzed by two conserved histidines in the active site (11).

Crystal structures of CPD photolyase have demonstrated that the FAD cofactor has an unusual U shape, with the isoalloxazine and adenine rings in close proximity (Fig. 3) (12–15). In addition, the DNA dimer is flipped out of the DNA helix and approaches the FAD cofactor (5, 16), but the distance between the DNA substrate and FAD cofactor is not certain. Theoretical studies (17–19), with one exception (20), have predicted that the distance between them precludes van der Waals

---

— 78 —

interactions. A long distance between FAD and the DNA substrate was also suggested by analysis of the electric dipole moment (21) and by EPR and electron nuclear double resonance (22). However, the crystal structure of CPD photolyase complexed with a CPD-like DNA lesion (15) showed a direct van der Waals contact of 3–4 Å between the cofactor and the thymine dimer (Fig. 3), a finding also supported by a femtosecond fluorescence and absorption spectroscopic study (23). Resonance Raman spectra have suggested that changes in the hydrogen bonding environment of the FAD cofactor in CPD photolyase after substrate binding (24) give rise to the increased redox potential of the FAD cofactor (25) and stabilize it in the catalytically active FADH⁻ state in the enzyme, but the precise alterations of the hydrogen bonding environments have not yet been determined. As for (6-4) photolyase, a crystal structure is not yet available. Although the high sequence homology between the two photolyases suggests that the interaction between the (6-4) photoproduct and the FAD cofactor may be similar to that between CPD and FAD in CPD photolyase, the quantum yield for (6-4) photolyase is much lower (0.05–0.1) than that for CPD photolyase (0.7–0.98).

Resonance Raman spectroscopy is a sensitive tool for probing the interactions between the flavin cofactor and its surroundings in flavoproteins (26, 27). To explore and compare the interactions between the damaged DNA and the FAD cofactor in (6-4) and CPD photolyases, we first constructed a His tag expression system to obtain adequate amounts of purified active enzymes. We then compared the resonance Raman

spectra for complexes of the neutral semiquinoid and oxidized forms with damaged DNA. Our results suggest that CPD interacts with both the benzene ring (Ring I) and the adenine ring of the FAD cofactor, whereas the (6-4) photoproduct interacts only with the adenine ring of the FAD cofactor. Such a structural difference may indicate different pathways of electron transfer for the two enzymes. In addition, the Raman spectra predict different substrate-induced changes in the hydrogen bonding environment for the two enzymes.

EXPERIMENTAL PROCEDURES

Enzyme Preparation—The gene of *Arabidopsis thaliana* (6-4) photolyase or *Escherichia coli* CPD photolyase was inserted at the NdeI and SacI sites of the pET-28a expression vector (Novagen). *E. coli* BL21(DE3) transformed with the vector was added to 0.5 liters of LB medium in a 3-liter flask and grown at 37 °C to A_{600} = 1.5. The culture was then cooled to 26 °C, adjusted to 0.2 mM isopropyl β-D-thiogalactopyranoside, incubated for 24 h, and then harvested by centrifugation. The pellet was frozen at −80 °C, thawed, resuspended in lysis buffer (20 mM sodium phosphate, 0.5 M NaCl, 1 mM dithiothreitol, and 5% glycerol, pH 7.4), and sonicated. Cell debris was removed from the lysate by ultracentrifugation at 40,000 rpm for 1 h. The cell-free extract was loaded onto a HisTrap HP column (Amersham Biosciences), and the fusion protein was eluted with elution buffer (20 mM sodium phosphate, 0.5 M NaCl, and 0.5 M imidazole, pH 7.4). Next, the sample was applied to a HiTrap heparin HP column (Amersham Biosciences) and eluted with a linear gradient of 0.3–1 M NaCl. A 2-liter culture of *E. coli* culture yielded ~12 mg of (6-4) photolyase and 10 mg of CPD photolyase. The N-terminal His tag was not removed from the fusion protein.

To prepare the fully oxidized enzyme from the purified sample, (6-4) photolyase was exposed to air for >48 h and then applied to a HiLoad 16/60 Superdex 200 prep grade column (Amersham Biosciences). Because the oxidization of CPD photolyase by air is very ineffective, the neutral semiquinoid FAD cofactor was removed by decreasing the pH, after which CPD photolyase was reconstituted with oxidized FAD (Sigma). All steps were performed according to the procedure described by Jorns *et al.* (28), except that the dithiothreitol was removed from the buffer, and a HiTrap phenyl FF (high sub) column (Amersham Biosciences) was used to remove excess FAD.

The purified enzyme was stored in 20 mM sodium phosphate, pH 7.4, containing 0.5 M NaCl. 10% glycerol was also added to stabilize the reconstituted CPD photolyase. The purity of the protein after application to the heparin column was determined by SDS-PAGE, and the monomeric form was identified by gel filtration chromatography on the HiLoad 16/60 Superdex 200 prep grade column. The concentration of the oxidized form of the enzyme was estimated based on the FAD absorbance at 450 nm (ϵ_{450} = $1.12 \times 10^4 \, M^{-1} cm^{-1}$) (29), and that
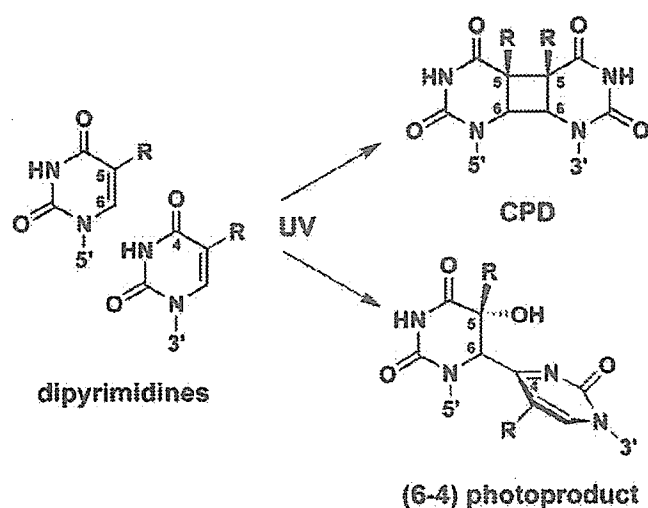

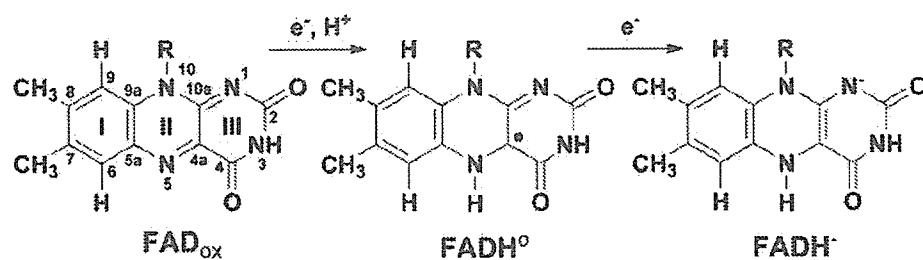FIGURE 1. **Structures of the UV-induced DNA lesions.** *R*, H or CH₃.

FIGURE 2. **Redox states and numbering scheme for the isoalloxazine ring of FAD in photolyase.**
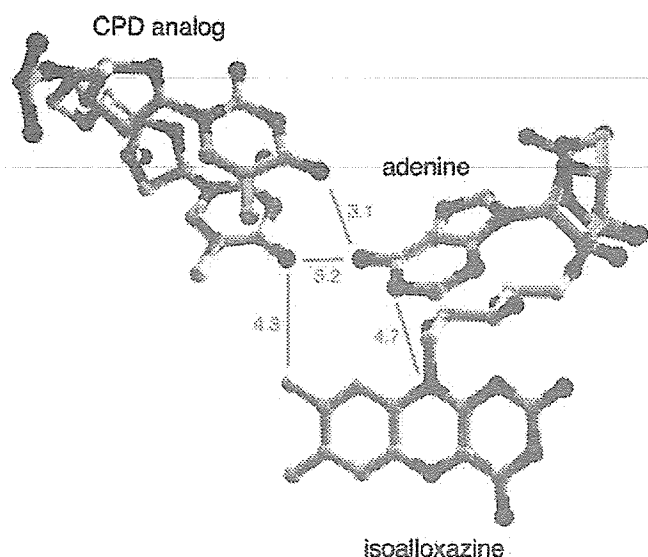
— 79 —

CPD analog

adenine

isoalloxazine

FIGURE 3. **Structure of the FAD cofactor and a CPD-like DNA lesion in CPD photolyase (Protein Data Bank code 1TEZ).** The distances of possible interactions are given in angstroms.

FIGURE 4. **Time course of absorption change in UV-damaged oligo(dT)$_8$ upon near UV-visible light irradiation in the presence of (6-4) photolyase (A) and CPD photolyase (B).** The absorbance at 266 nm (O) is due to undamaged DNA, and that at 325 nm ($\triangle$) is due to the (6-4) photoproduct.

of the neutral semiquinoid form was estimated from the absorbance at 580 nm ($\epsilon_{580} = 4.8 \times 10^3$ M^{-1} cm^{-1}) (30).

Substrate Preparation—The substrate was prepared by irradiation of oligothymine (oligo(dT)$_8$ or oligo(dT)$_{10}$; Operon Biotechnologies) for 30 min with 254 nm UV light (6.4 milliwatt/cm^2) using a UV transilluminator (TFX-20-MC, Vilber Lourmat). The sample was loaded in a cylindrical spinning cell that was cooled during the UV irradiation by flushing with cold N$_2$ gas passed through liquid N$_2$. Formation of dimers was monitored by the decrease in the monomer absorption band at 266 nm and the appearance of an absorption band of the (6-4) photoproduct at 325 nm (31).

Enzyme Activity—The enzyme activity of the His-tagged (6-4) and CPD photolyases was measured using a method based on the assay for CPD photolyase (32). Briefly, a complex of 2 μM photolyase and 50 μM UV-irradiated oligo(dT)$_8$ in 50 mM Tris-HCl, pH 7.4, 200 mM NaCl, and 1 mM dithiothreitol was placed in a spinning cell and illuminated with a tungsten light (PHL-150, Sigma Koki Co., Ltd.) at room temperature. The UV-visible absorption spectrum of the sample was measured as a function of time.

Absorption and Resonance Raman Spectroscopy—Optical absorption spectra of samples were recorded with a Hitachi UV-3310 UV-visible spectrophotometer at room temperature. Resonance Raman spectra were obtained with a single monochromator (SPEX750M, Jobin Yvon) equipped with a liquid N$_2$-cooled CCD detector (Spec10:400B/LN, Roper Scientific, Inc.). The excitation wavelengths were 568.2 and 488.0 nm from a krypton/argon mixed-gas ion laser (BeamLok 2060, Spectra-Physics) for the semiquinoid and oxidized forms, respectively. The laser power at the sample point was 5 milliwatts. Rayleigh scattering was removed with appropriate holographic notch filters (Kaiser Optical Systems). Raman shifts were calibrated with indene, and the accuracy of the peak positions of the well defined Raman bands was ± 1 cm^{-1}.
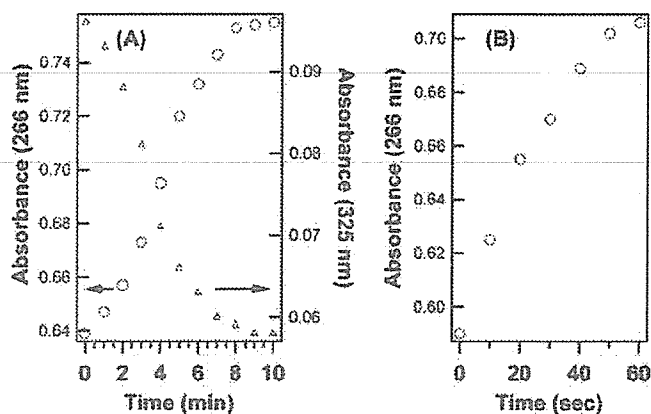
For the semiquinoid form, the measurements were made using an aliquot of 150 μM enzyme in 20 mM sodium phosphate buffer, pH 7.4, containing 0.5 M NaCl. For the oxidized form, the buffer was the same, but the enzyme concentration was 75 μM, and 10% glycerol was added for CPD photolyase. A 2-fold excess of oligo(dT)$_{10}$ or UV-irradiated oligo(dT)$_{10}$ was added to the mixture. All measurements were performed with a spinning Raman cell containing 80 μl of sample solution, and all samples were cooled with cold N$_2$ gas. The structureless background in the raw spectrum was removed by a polynomial subtraction procedure using Igor Pro 5.03 (WaveMetrics). The resonance Raman spectra of oxidized CPD photolyase were normalized by the Raman band for glycerol in the buffer, so their differences both in frequency and intensity are reliable, whereas all the other Raman data were normalized by their most intense band presumably. Thus, only the differences in frequencies were considered.

RESULTS

Enzyme Activity—The time course curves for dimer repair by 2 μM (6-4) and CPD photolyases in the presence of 50 μM UV-damaged oligo(dT)$_8$ are shown in Fig. 4 (A and B, respectively). UV damage substantially reduced the 266 nm band of undamaged DNA and resulted in the appearance of a significant 325 nm band for the (6-4) photoproduct. Illumination of the damaged DNA complex with white light in the presence of (6-4) or CPD photolyase resulted in the gradual reappearance of the 266 nm band and, for the (6-4) photolyase, the disappearance of the 325 nm band. Therefore, although the enzymes used here have N-terminal His tags, they are catalytically active.

Absorption Spectra of Photolyase Complexed with DNA Lesions—Immediately after purification, most of the (6-4) and CPD photolyases were in the neutral semiquinoid form with FADH° (Fig. 5, A and C, respectively). The absorption spectra for the fully oxidized (6-4) and CPD photolyases with FAD$_{ox}$ are shown in Fig. 5 (B and D), respectively. Also shown are the spectra of the enzyme-substrate complexes with (*dotted lines*) and without (*solid lines*) substrate. The absorbance maxima of FADH° (586 and 623 nm) and FAD$_{ox}$ (380 nm) in CPD photolyase were significantly shifted upon
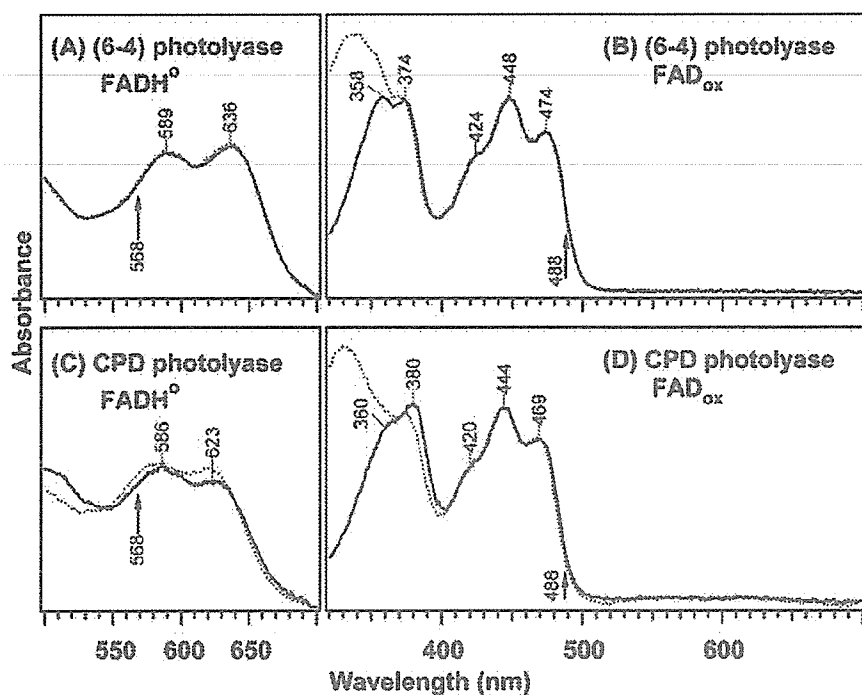
—80—

FIGURE 5. **Absorption spectra of (6-4) and CPD photolyases in the absence (*solid lines*) and presence (*dotted lines*) of UV-irradiated oligo(dT)$_{10}$.** *A*, neutral semiquinoid (6-4) photolyase; *B*, oxidized (6-4) photolyase; *C*, neutral semiquinoid CPD photolyase; *D*, oxidized CPD photolyase. The *arrows* indicate the Raman excitation wavelengths.

that undamaged DNA does not interact with the active site in either photolyase.

The band near 1606 cm^{-1} in photolyases is a marker for the neutral semiquinoid flavin (33). Recent Raman studies suggested that there are two closely overlapping modes in the frequency region of this marker band and that, in fact, splitting of this band can be observed for the D$_2$O substitution (24, 34). The higher frequency counterpart arises from the stretching of Ring I, and the lower frequency counterpart comes from the C–C/C–N(5) stretching and N(5)–H bending of Ring II (Fig. 2) (24, 34, 35). Upon substrate binding to CPD photolyase, there was a significant downshift in the frequency of this marker band. However, this shift was not detected for the (6-4) photolyase. The 1528 cm^{-1} band of CPD photolyase, which is assigned to the C–C/C–N(5) stretching of Ring II and thought to be a sensitive indicator of hydrogen bonding to N(5)–H of flavin (34), was upshifted, but this was not observed for (6-4) photolyase. The 1398 cm^{-1} band of (6-4) photolyase and the corresponding band of CPD photolyase at 1391 cm^{-1}, which are tentatively assigned to the C–N(10) stretching (34), were both upshifted. The 1338 cm^{-1} band of (6-4) photolyase seemed to be unaltered by substrate binding, whereas the bands of both enzymes at 1331 cm^{-1} seemed to be less intensified in the substrate-bound form (Fig. 6A). The sensitivity of this band to deuterium exchange indicates that it may be influenced by perturbations in the hydrogen bonding environment of the flavin ring (24). The 1298 and 1302 cm^{-1} bands, which are assigned to C–N(5) stretching (34), were upshifted only in CPD photolyase.

These substrate-induced frequency shifts of FADH° in (6-4) and CPD photolyases are summarized and quantitatively compared in Table 1. The frequency changes in CPD photolyase were much larger than those in (6-4) photolyase, and the results are compatible with the changes in the absorption spectra upon substrate binding (Fig. 5). Notably, the shifts of the Raman bands at 1606 and 1607 cm^{-1} were the most different, indicating different interactions of UV-damaged DNA with FADH° in the two photolyases.

Resonance Raman Spectra of Oxidized Photolyase Complexed with DNA Lesions—The vibrational assignments are much better established for the oxidized flavin than for the neutral semiquinoid form (35–38). Like the semiquinoid flavin, the oxidized flavin has a planar conformation (39) and should undergo a similar structural change upon substrate binding. Therefore, investigation of the oxidized enzymes could enhance the

binding of the UV-damaged DNA.[5] This blue shift is in agreement with previous findings (24, 28). In contrast, substrate binding had little effect on the absorption spectra of (6-4) photolyase.

The absorption maxima around 590 and 630 nm in Fig. 5 (*A* and *C*) are due to the electronic transition of FADH°. These absorption maxima are absent from the spectra for FAD$_{ox}$ (Fig. 5, *B* and *D*). In accordance with these absorption spectra, we chose 568.2 and 488.0 nm as the Raman excitation wavelengths to selectively enhance the neutral semiquinoid and oxidized forms, respectively (Fig. 5, *arrows*).

Resonance Raman Spectra of Neutral Semiquinoid Photolyase Complexed with DNA Lesions—The resonance Raman spectra of the neutral semiquinoid (6-4) and CPD photolyases are shown in Fig. 6 (*A* and *B*, respectively). Fig. 6 shows the spectra for the enzyme alone (*traces a*), with undamaged DNA (*traces b*), and with UV-damaged DNA (*traces c*). Some clear peaks are evident in the difference spectra between the enzyme alone and the enzyme·UV-irradiated DNA complex (*traces e*) but not in the difference spectra between the enzyme alone and the enzyme·undamaged DNA complex (*traces d*). These results were repeated in independent experiments, and they suggest that the structure and environment of the FAD cofactor change in both photolyases upon binding of a specific substrate and

---

[5] The prominent near-UV absorption maximum around 340 nm shown as a *dotted line* arises from the UV-damaged DNA of the (6-4) photoproduct (31). The presence of this band, as well as the invariable frequencies of all absorption bands before and after Raman measurement (data not shown), indicates the presence of an adequate amount of UV-damaged DNA substrate in this study.
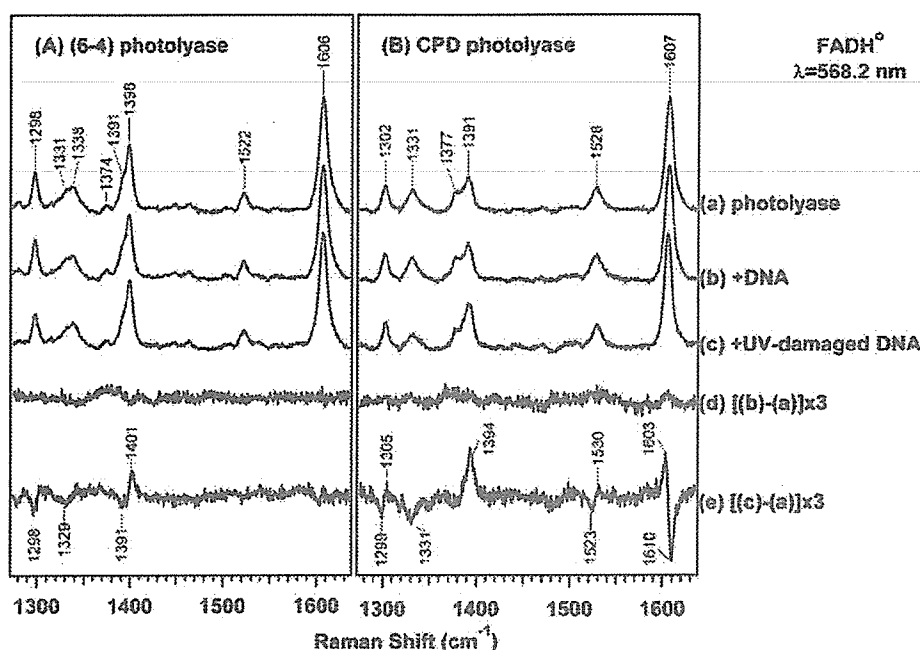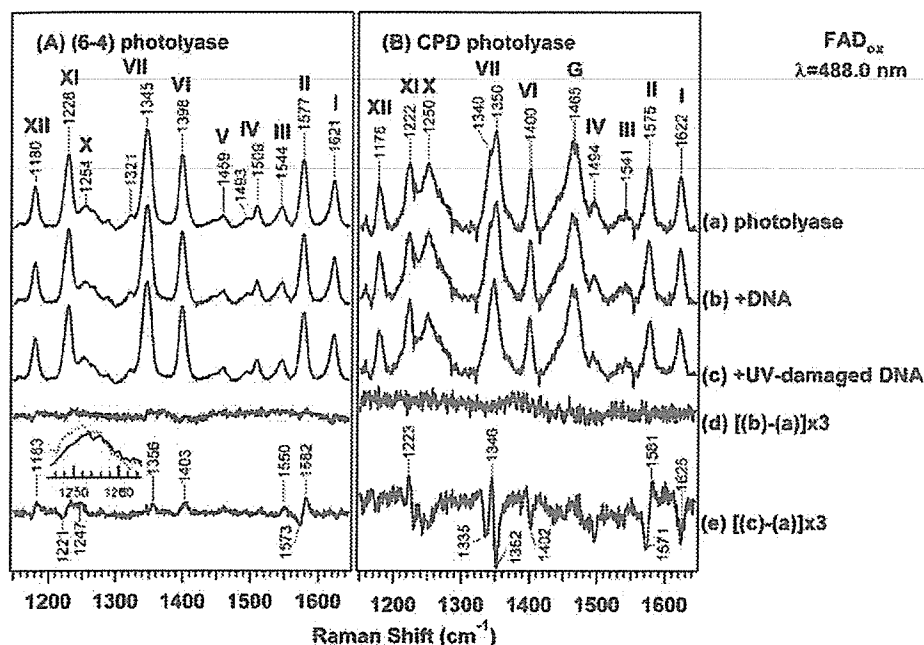
FIGURE 7. **Resonance Raman spectra of 75 μM oxidized (6-4) photolyase (A) and CPD photolyase (B).** In *A* and *B*, *trace a* shows the spectrum for enzyme alone; *trace b* shows the spectrum in the presence of 150 μM oligo(dT)$_{10}$; *trace c* shows the spectrum in the presence of 150 μM UV-irradiated oligo(dT)$_{10}$; *trace d* shows the difference spectrum for (*trace b* – *trace a*) × 3; and *trace e* shows the difference spectrum for (*trace c* – *trace a*) × 3. The Raman excitation wavelength was 488.0 nm. Band numbering is according to Ref. 36. G indicates the Raman band of glycerol. *Inset*, band X of (6-4) photolyase in the absence (*solid line*) and presence (*dotted line*) of UV-irradiated oligo(dT)$_{10}$.

TABLE 2

Raman frequency shifts of FAD$_{ox}$ in (6-4) and CPD photolyases upon substrate binding

Band	FAD$_{ox}$ in (6-4) photolyase		FAD$_{ox}$ in CPD photolyase	
	Mode	Frequency shift	Mode	Frequency shift
	cm^{-1}		*cm^{-1}*	
I	1621	0	1622	−2
II	1577	+1	1575	+2
VI	1398	<+1	1400	<−1
VII	1345	<+1	1350, 1340	−3, +7
X	1254	−1	1250	0
XI	1228	< 1	1222	<1
XII	1180	<−1	1178	0

photolyase was significantly downshifted upon substrate binding, whereas the corresponding band in (6-4) photolyase was unaltered. This band is thought to be composed of two overlapping modes, *viz.* vibration of Ring I and the C–C/C–N(5)/N(5)–H coupled mode of Ring II. Nishina *et al.* (40) have reported that this marker band in a neutral semiquinoid riboflavin is insensitive to isotopic substitution of the carbon and nitrogen atoms in Rings II and III of flavin, indicating that the vibrations of Ring I are the major contributors to this band. This is also supported by our theoretical assignment of the neutral semiquinoid flavin.[6] Furthermore, the resonance Raman spectra in Fig. 7 show that band I, which arises from the Ring I stretching of the oxidized flavin, was downshifted only in CPD photolyase upon substrate binding (Table 2). Therefore, the alterations of the Ring I vibrations of the isoalloxazine ring

[6] Li, J., Uchida, T., Ohta, T., Todo, T., and Kitagawa, T. (June 28, 2006) *J. Phys. Chem. B* 10.1021/jp062998b, submitted for publication.

caused the significant downshifts of the bands at 1607 cm^{-1} of FADH° and 1622 cm^{-1} of FAD$_{ox}$ in CPD photolyase. These Raman spectral features indicate that Ring I of the FAD cofactor interacts with the damaged DNA upon substrate binding in CPD photolyase but not in (6-4) photolyase.

The absorption spectrum of CPD photolyase shows a larger blue shift upon substrate binding compared with the spectrum of (6-4) photolyase (Fig. 5). The apparent blue shift of the absorption band at 380 nm for FAD$_{ox}$ in CPD photolyase may indicate a decreased polarity around the isoalloxazine ring because such a shift is also observed for flavin when the solvent is changed from polar to non-polar (41). The difference Raman spectrum of FAD$_{ox}$ in CPD photolyase, which was normalized by the solvent band of glycerol, shows a downshift and decrease in intensity of band I as indicated by a negative band at 1625 cm^{-1} in the difference spectrum (Fig. 7B, *trace e*). Such a change in band I in the oxidized flavin is observed when the polarity of its surroundings is reduced (42, 43). Therefore, the downshifts of the Raman bands at 1607 cm^{-1} of FADH° and 1622 cm^{-1} of FAD$_{ox}$ appear to reflect a decrease in the polarity around the isoalloxazine ring when the pyrimidine bases of CPD approach. Specifically, there is a stronger hydrophobic interaction between CPD and Ring I of isoalloxazine. The hydrophobic interaction has been identified to have the same range as the van der Waals dispersion force (44). Therefore, CPD and Ring I of isoalloxazine in CPD photolyase may make a direct van der Waals contact (~4 Å), a possibility also suggested by the crystal structure of CPD photolyase containing a substrate analog (Fig. 3) (15). MacFarlane and Stanley (21) showed that the electric dipole moment of CPD is responsible for the electrochromic shift of the electronic transition energy of FAD$_{ox}$ in CPD photolyase, and they estimated a distance of 5.5–8 Å between CPD and FAD. In a later report (45), they reduced this distance because they observed a very high rate of electron transfer. The absorption spectra upon substrate binding show less of a blue shift in the absorption bands for (6-4) photolyase than for CPD photolyase (Fig. 5). This smaller change in electronic transition energy induced by damaged DNA indicates a greater distance between the (6-4) photoproduct and the FAD cofactor in (6-4) photolyase. Fig. 8 shows a schematic illustration of the differences between the positions of DNA lesions and the isoalloxazine ring in the FAD cofactor for the two photolyases.

Interactions between UV-damaged DNA and the Adenine Ring of FAD—Upon substrate binding, the band at 1391 cm^{-1} observed for FADH° in CPD photolyase was upshifted (Fig. 6).
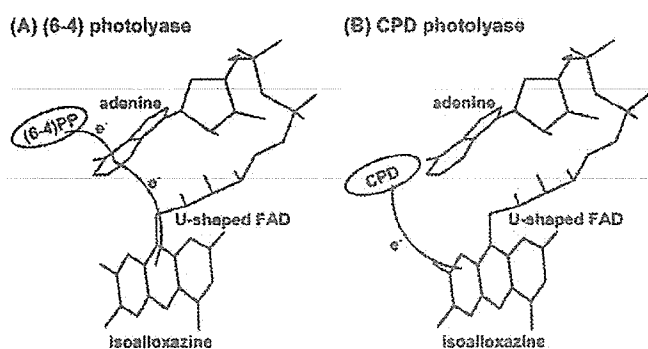
— 83 —

(A) (6-4) photolyase

(B) CPD photolyase

FIGURE 8. **Schematic illustration of the positions of a substrate and the putative electron transfer pathways in (6-4) photolyase (A) and CPD photolyase (B).** *(6-4)PP,* (6-4) photoproduct.

We have proposed that this mode is derived mainly from the stretching of the N(10)–C(10a) bond in the isoalloxazine ring.[6] The x-ray crystal structure of CPD photolyase revealed that the FAD cofactor has a unique U shape, in which an adenine ring approaches the isoalloxazine ring near the N(10)–C(10a) moiety (12–15). Therefore, the upshift of the 1391 cm^{-1} band appears to arise from the alteration of the ring stacking conformation between adenine and isoalloxazine rings. Furthermore, the pyrimidine bases of the CPD analog engage in hydrogen bonding interactions with the adenine ring of the FAD cofactor as shown in Fig. 3. Accordingly, a change in ring stacking upon substrate binding is expected because of alterations of the hydrogen bonding interactions between the substrate and the adenine ring of the FAD cofactor, resulting in an upshift of the 1391 cm^{-1} band. The 1398 cm^{-1} band of (6-4) photolyase was also upshifted. Because the FAD-binding domains of (6-4) and CPD photolyases are closely related (46), a similar conformational change is also expected to occur in (6-4) photolyase.

Band VII of the oxidized flavin, which is assigned to the stretching of N(10)–C(10a) and N(10)–C(1′) (ribityl), also reflects the vibrations of the N-10 atom. Therefore, this mode should also be sensitive to the U-shaped bending and ring stacking conformation of FAD. For (6-4) photolyase, this band was upshifted, and the split band VII in CPD photolyase merged into a single band upon substrate binding (Fig. 7). These alterations also supported the stronger interaction between the adenine ring and UV-damaged DNA (Fig. 8).

In (6-4) and CPD photolyases, band II (1577 and 1575 cm^{-1}, respectively) is at a significantly lower frequency compared with free FAD (1585 cm^{-1}) (47). The frequency of band II is known to be downshifted upon formation of a hydrogen bond at N-1 of flavin (38). N-1 and the 2′-OH of the ribityl chain are thought to form a strong hydrogen bond because of the U shape of the FAD cofactor in CPD photolyase (24). Therefore, the lower frequency of band II in (6-4) and CPD photolyases should reflect a U-shaped conformation of the FAD cofactor. An apparent upshift of band II upon substrate binding was identified for both enzymes (Fig. 7). This indicates the departure of the adenine ring from the isoalloxazine of FAD as a result of the hydrogen bonding interaction between adenine and the substrate.

Alterations in Hydrogen Bonding Interactions around FAD Induced by Substrate Binding—The crystal structure of CPD photolyase revealed that N(5)–H donates a hydrogen bond to an asparagine that is conserved in (6-4) photolyase. Fig. 6 shows that the Raman band at 1528 cm^{-1} in CPD photolyase was upshifted upon substrate binding, whereas that at 1522 cm^{-1} in (6-4) photolyase was unaltered. This band is a marker for hydrogen bonding at N(5)–H in the neutral semiquinoid flavin (34), and it has been empirically used in a Raman study of cytochrome P-450 reductase (48). Therefore, the upshift of the 1522 cm^{-1} band indicates that the hydrogen bond at N(5)–H of FADH° in CPD photolyase is weakened when the enzyme is bound to CPD. This Raman prediction is also supported by the more sensitive band at 1302 cm^{-1} in CPD photolyase, which involves C–N(5) stretching (Fig. 6 and Table 1).

Another hydrogen bonding interaction may be formed at N(3)–H in both FADH° and FAD$_{ox}$. Band X of the oxidized flavin at 1254 cm^{-1}, which reflects C–N(3) stretching and N(3)–H bending, seemed to be downshifted in (6-4) photolyase (Fig. 7 and Table 2), indicating that the hydrogen bond would be weakened by substrate binding. The slight frequency shifts of bands VI, XI, and XII in both enzymes (Fig. 7 and Table 2) may also reflect the alterations of the hydrogen bonding environment or vibrations of Ring I induced by substrate binding. On the other hand, the Raman bands of FADH° at 1338 and 1331 cm^{-1} in (6-4) photolyase approach the profile of the single band at 1331 cm^{-1} in CPD photolyase. The lower frequency of band X suggests that the hydrogen bond at N(3)–H in CPD photolyase is weaker than that in (6-4) photolyase; therefore, the hydrogen bond at N(3)–H in (6-4) photolyase may be weakened upon substrate binding.

Implication for Biological Functions—Although the crystal structure of CPD photolyase shows that Ring I is in the direction of the DNA lesion (15), previous studies revealed a lower density for unpaired electrons and approximately for the whole electrons on Ring I of the semiquinoid flavin radical, suggesting that electron transfer between the isoalloxazine ring and CPD is not direct (49–51). It was assumed that the adenine ring of the U-shaped FAD fills the gap between the isoalloxazine ring and damaged DNA and provides effective coupling between them (20); however, a recent study using femtosecond absorption spectroscopy concluded that there is a direct electron transfer from FAD to CPD because intramolecular electron transfer could not be observed in the absence of substrate (23). Our Raman study also suggests that CPD makes a direct contact with Ring I of the isoalloxazine ring within a van der Waals distance and that it interacts with the adenine ring. Therefore, our results support a direct electron transfer from the flavin ring to CPD in CPD photolyase, although modulation of the electron transfer by the adenine ring cannot be ruled out. In contrast, in (6-4) photolyase, the (6-4) photoproduct is located slightly farther from the flavin ring and does not come into contact with it. This indicates that electron transfer in (6-4) photolyase from the flavin ring to the (6-4) photoproduct via the bridged adenine ring is more likely than a direct transfer. The putative electron transfer pathways in (6-4) and CPD photolyases are illustrated in Fig. 8.

— 84 —

The hydrogen bonding environment is an important factor controlling the redox potential of flavin in flavoproteins (52). In a study on the control of the redox potential of flavodoxin, introduction of a β-branched threonine side chain at position 57 was shown to change the protein environment of the isoalloxazine ring of FMN, and hydrogen bonding at N(5)–H of flavin was expected to be weaker than in the native enzyme based on the lower pK_a value of N(5)–H. This modification of the hydrogen bonding structure of the flavin ring is expected to lead to a significant increase in the redox potential for the semiquinone-hydroquinone couple (53). Furthermore, molecular orbital calculations showed that the weakened hydrogen bond at donor positions (N(3)–H and N(5)–H) would decrease the lowest unoccupied molecular orbital energy (54–56). This would enhance the electron acceptability, increasing the redox potential of flavin. In this study, we confirmed that the hydrogen bond at N(5)–H of FAD in CPD photolyase is weakened upon substrate binding. Therefore, weakening of the hydrogen bond at N(5)–H by perturbation of the active site upon binding of CPD is expected to increase the redox potential of the CPD photolyase·substrate complex (25). In photolyases, FADH° is generated during DNA repair and must be reduced to FADH$^-$ before the next catalytic cycle. Such an increase in the redox potential upon CPD binding is in favor of the reverse electron transfer from the repaired DNA to FADH° as well as the high quantum yield for CPD photolyase. Similarly, a weakened hydrogen bond at N(3)-H in (6-4) photolyase may also decrease the lowest unoccupied molecular orbital energy and facilitate the reduction of FADH°.

An active photolyase is in an anionic fully reduced form. However, we have no data on the reduced enzyme because its complex with the substrate is not so stable that the UV-damaged DNA is easily repaired by the probe light during resonance Raman measurements. Anionic reduced flavin and neutral semiquinoid and oxidized flavins are planar (39), and the FAD cofactors in the latter two redox states have been suggested to contact the substrate similarly according to our Raman spectra. In addition, the flipping of CPD out of the DNA helix into the active-site cavity has been revealed to be independent of the redox states of the FAD cofactor by fluorescence study on oxidized and fully reduced CPD photolyases (16). Therefore, the interactions between substrate and FAD cofactor observed in this work were supposed to occur in the fully reduced enzyme, too.

Conclusion—In this study, we reported UV-visible absorption and resonance Raman spectra of the neutral semiquinoid and oxidized (6-4) and CPD photolyases as well as their changes upon substrate binding. We demonstrated that a direct hydrophobic interaction may occur between CPD and Ring I of FAD in CPD photolyase but that this does not occur for (6-4) photolyase, indicating that the electron transfer mechanisms in these two enzymes may be different. Another hydrogen bond may be formed between UV-damaged DNA and the adenine ring of FAD in both enzymes upon substrate binding. The substrate may also weaken the hydrogen bond at N(5)–H in CPD photolyase and at N(3)–H in (6-4) photolyase. The former change could explain the increased redox potential of FAD recently observed in CPD photolyase. These findings should help establish the structure of the DNA·FAD complex and the mechanism by which substrate binding modulates both enzymes.

REFERENCES

1. Lindahl, T. (1993) *Nature* 362, 709–715
2. Sancar, A. (1994) *Biochemistry* 33, 2–9
3. Todo, T., Takemori, H., Ryo, H., Ihara, M., Matsunaga, T., Nikaido, O., Sato, K., and Nomura, T. (1993) *Nature* 361, 371–374
4. Sancar, A. (2003) *Chem. Rev.* 103, 2203–2237
5. Zhao, X. D., Liu, J. Q., Hsu, D. S., Zhao, S. Y., Taylor, J. S., and Sancar, A. (1997) *J. Biol. Chem.* 272, 32580–32590
6. Hitomi, K., Kim, S. T., Iwai, S., Harima, N., Otoshi, E., Ikenaga, M., and Todo, T. (1997) *J. Biol. Chem.* 272, 32591–32598
7. Sancar, G. B., Jorns, M. S., Payne, G., Fluke, D. J., Rupert, C. S., and Sancar, A. (1987) *J. Biol. Chem.* 262, 492–498
8. Cichon, M. K., Arnold, S., and Carell, T. (2002) *Angew. Chem. Int. Ed. Engl.* 41, 767–770
9. Todo, T., Ryo, H., Yamamoto, K., Toh, H., Inui, T., Ayaki, H., Nomura, T., and Ikenaga, M. (1996) *Science* 272, 109–112
10. Kim, S. T., Malhotra, K., Smith, C. A., Taylor, J. S., and Sancar, A. (1994) *J. Biol. Chem.* 269, 8535–8540
11. Hitomi, K., Nakamura, H., Kim, S. T., Mizukoshi, T., Ishikawa, T., Iwai, S., and Todo, T. (2001) *J. Biol. Chem.* 276, 10103–10109
12. Park, H. W., Kim, S. T., Sancar, A., and Deisenhofer, J. (1995) *Science* 268, 1866–1872
13. Tamada, T., Kitadokoro, K., Higuchi, Y., Inaka, K., Yasui, A., deRuiter, P. E., Eker, A. P. M., and Miki, K. (1997) *Nat. Struct. Biol.* 4, 887–891
14. Komori, H., Masui, R., Kuramitsu, S., Yokoyama, S., Shibata, T., Inoue, Y., and Miki, K. (2001) *Proc. Natl. Acad. Sci. U. S. A.* 98, 13560–13565
15. Mees, A., Klar, T., Gnau, P., Hennecke, U., Eker, A. P. M., Carell, T., and Essen, L. O. (2004) *Science* 306, 1789–1793
16. Christine, K. S., MacFarlane, A. W., Yang, K. S., and Stanley, R. J. (2002) *J. Biol. Chem.* 277, 38339–38344
17. Hahn, J., Michel-Beyerle, M. E., and Rosch, N. (1998) *J. Mol. Model.* 4, 73–82
18. Sanders, D. B., and Wiest, O. (1999) *J. Am. Chem. Soc.* 121, 5127–5134
19. Hahn, J., Michel-Beyerle, M. E., and Rosch, N. (1999) *J. Phys. Chem. B* 103, 2001–2007
20. Antony, J., Medvedev, D. M., and Stuchebrukhov, A. A. (2000) *J. Am. Chem. Soc.* 122, 1057–1065
21. MacFarlane, A. W., and Stanley, R. J. (2001) *Biochemistry* 40, 15203–15214
22. Weber, S., Richter, G., Schleicher, E., Bacher, A., Mobius, K., and Kay, C. W. M. (2001) *Biophys. J.* 81, 1195–1204
23. Kao, Y. T., Saxena, C., Wang, L. J., Sancar, A., and Zhong, D. P. (2005) *Proc. Natl. Acad. Sci. U. S. A.* 102, 16128–16132
24. Schelvis, J. P. M., Ramsey, M., Sokolova, O., Tavares, C., Cecala, C., Connell, K., Wagner, S., and Gindt, Y. M. (2003) *J. Phys. Chem. B* 107, 12352–12362
25. Gindt, Y. M., Schelvis, J. P. M., Thoren, K. L., and Huang, T. H. (2005) *J. Am. Chem. Soc.* 127, 10472–10473
26. Morris, M. D., and Bienstock, R. J. (1986) in *Advances in Spectroscopy* (Clark, R. J. H., and Hester, R. E., eds.) Vol. 13, John Wiley & Sons, Inc., New York
27. McFarland, J. T. (1987) in *Biological Applications of Raman Spectroscopy* (Spiro, T. G., ed) Vol. 2, John Wiley & Sons, Inc., New York
28. Jorns, M. S., Wang, B. Y., Jordan, S. P., and Chanderkar, L. P. (1990) *Biochemistry* 29, 552–561
29. Todo, T., Kim, S. T., Hitomi, K., Otoshi, E., Inui, T., Morioka, H., Kobayashi, H., Ohtsuka, E., Toh, H., and Ikenaga, M. (1997) *Nucleic Acids Res.* 25, 764–768
30. Wang, B. Y., and Jorns, M. S. (1989) *Biochemistry* 28, 1148–1152

— 85 —

31. Franklin, W. A., Lo, K. M., and Haseltine, W. A. (1982) *J. Biol. Chem.* 257, 13535–13543
32. Jorns, M. S., Sancar, G. B., and Sancar, A. (1985) *Biochemistry* 24, 1856–1861
33. Nishina, Y., Shiga, K., Horiike, K., Tojo, H., Kasai, S., Matsui, K., Watari, H., and Yamano, T. (1980) *J. Biochem. (Tokyo)* 88, 411–416
34. Murgida, D. H., Schleicher, E., Bacher, A., Richter, G., and Hildebrandt, P. (2001) *J. Raman Spectrosc.* 32, 551–556
35. Zheng, Y. G., Dong, J., Palfey, B. A., and Carey, P. R. (1999) *Biochemistry* 38, 16727–16732
36. Bowman, W. D., and Spiro, T. G. (1981) *Biochemistry* 20, 3313–3318
37. Abe, M., and Kyogoku, Y. (1987) *Spectrochim. Acta Part A Mol. Biomol. Spectrosc.* 43, 1027–1037
38. Lively, C. R., and McFarland, J. T. (1990) *J. Phys. Chem.* 94, 3980–3994
39. Zheng, Y. J., and Ornstein, R. L. (1996) *J. Am. Chem. Soc.* 118, 9402–9408
40. Nishina, Y., Shiga, K., Miura, R., Tojo, H., Ohta, M., Miyake, Y., Yamano, T., and Watari, H. (1983) *J. Biochem. (Tokyo)* 94, 1979–1990
41. Yagi, K., Ohishi, N., Nishimoto, K., Choi, J. D., and Song, P. S. (1980) *Biochemistry* 19, 1553–1557
42. Schmidt, J., Coudron, P., Thompson, A. W., Watters, K. L., and McFarland, J. T. (1983) *Biochemistry* 22, 76–84
43. Muller, F., Vervoort, J., Lee, J., Horowitz, M., and Carreira, L. A. (1983) *J. Raman Spectrosc.* 14, 106–117
44. Israelachvili, J., and Pashley, R. (1982) *Nature* 300, 341–342
45. MacFarlane, A. W., and Stanley, R. J. (2003) *Biochemistry* 42, 8558–8568
46. Todo, T. (1999) *Mutat. Res.* 434, 89–97
47. Benecky, M., Li, T. Y., Schmidt, J., Frerman, F., Watters, K. L., and McFarland, J. (1979) *Biochemistry* 18, 3471–3476
48. Sugiyama, T., Nisimoto, Y., Mason, H. S., and Loehr, T. M. (1985) *Biochemistry* 24, 3012–3019
49. Kay, C. W. M., Feicht, R., Schulz, K., Sadewater, P., Sancar, A., Bacher, A., Mobius, K., Richter, G., and Weber, S. (1999) *Biochemistry* 38, 16740–16748
50. Weber, S., Mobius, K., Richter, G., and Kay, C. W. (2001) *J. Am. Chem. Soc.* 123, 3790–3798
51. Weber, S. (2005) *Biochim. Biophys. Acta* 1707, 1–23
52. Miura, R. (2001) *Chem. Rec.* 1, 183–194
53. Ludwig, M. L., Pattridge, K. A., Metzger, A. L., Dixon, M. M., Eren, M., Feng, Y. C., and Swenson, R. P. (1997) *Biochemistry* 36, 1259–1280
54. Nishimoto, K., Fukunaga, H., and Yagi, K. (1986) *J. Biochem. (Tokyo)* 100, 1647–1653
55. Nishimoto, K., Kai, E., and Yagi, K. (1984) *Biochim. Biophys. Acta* 802, 321–325
56. Yagi, K. (1987) *Chem. Scr.* 27A, 27–30

— 86 —

Characteristic Structure and Environment in FAD Cofactor of (6−4) Photolyase along Function Revealed by Resonance Raman Spectroscopy

Jiang Li,[†,‡] Takeshi Uchida,[†,‡,||] Takehiro Ohta,[†,⊥] Takeshi Todo,[§] and Teizo Kitagawa*[†,‡,⊽]

Okazaki Institute for Integrative Bioscience, National Institutes of Natural Sciences. Myodaiji, Okazaki, Aichi 444-8787, Japan, Department of Photoscience, School of Advanced Sciences, Graduate University for Advanced Studies, Shonan Village, Hayama, Kanagawa, 240-0193, Japan, and Radiation Biology Center, Kyoto University. Yoshidakonoe-cho, Sakyo-ku, Kyoto, 606-8501, Japan

Received: May 16, 2006

A pyrimidine−pyrimidone (6−4) photoproduct and a cyclobutane pyrimidine dimer (CPD) are major DNA lesions induced by ultraviolet irradiation, and (6−4) photolyase, an enzyme with flavin adenine dinucleotide (FAD) as a cofactor, repairs the former specifically by light illumination. We investigated resonance Raman spectra of (6−4) photolyase from *Arabidopsis thaliana* having neutral semiquinoid and oxidized forms of FAD, which were selectively intensity enhanced by excitations at 568.2 and 488.0 nm, respectively. DFT calculations were carried out for the first time on the neutral semiquinone. The marker band of a neutral semiquinone at 1606 cm^{-1} in H_2O, whose frequency is the lowest among various flavoenzymes, apparently splits into two comparable bands at 1594 and 1608 cm^{-1} in D_2O, and similarly, that at 1522 cm^{-1} in H_2O does into three bands at 1456, 1508, and 1536 cm^{-1} in D_2O. This D_2O effect was recognized only after being oxidized once and photoreduced to form a semiquinone again, but not by simple H/D exchange of solvent. Some Raman bands of the oxidized form were observed at significantly low frequencies (1621, 1576 cm^{-1}) and with band splittings (1508/1493, 1346/1320 cm^{-1}). These Raman spectral characteristics indicate strong H-bonding interactions (at N5−H, N1), a fairly hydrophobic environment, and an electron-lacking feature in benzene ring of the FAD cofactor, which seems to specifically control the reactivity of (6−4) photolyase.

Introduction

Ultraviolet (UV) light irradiation to organisms causes damages of cellular DNA by forming a dimer between adjacent pyrimidine bases, which can result in mutation, cell death, and cancer afterward.[1] Most of the damaged DNA is cyclobutane pyrimidine dimer (CPD) and (6−4) photoproduct, which are repaired by CPD photolyase and (6−4) photolyase, respectively, under illumination by near-UV/visible light.[2,3]

For CPD photolyase, structure and mechanism of the enzymatic reaction have been extensively studied. The resting CPD photolyase contains an anionic fully reduced FAD (FADH$^-$) as an essential cofactor and also either 5,10-methenyltetrahydrofolate polyglutamate (MTHF) or flavin derivative as a light-harvesting chromophore.[4] Crystal structures of CPD photolyase have demonstrated that the FAD cofactor, which is located in a deeply buried pocket within a protein matrix and held by the conserved residues through direct contacts, adopts an unusual and unique U-shaped conformation of isoalloxazine with an adenine ring in close proximity.[5−8] The latest crystal structure of CPD photolyase complexed with a CPD-like DNA lesion shows that the adenine ring of FAD bridges the electron-donating isoalloxazine ring and the electron-

accepting substrate.[8] The proposed repair mechanism of CPD photolyase is as follows: after recognizing and binding to CPD, the light-harvesting chromophore or FADH$^-$ absorbs a photon, and then, its excited state, FADH$^-$*, is formed either directly or by energy transfer from a light-harvesting chromophore. Next, FADH$^-$* transfers an electron to the CPD, which splits it into two pyrimidine monomers, and then, FADH$^-$* is converted into a neutral semiquinoid form (FADH°). Finally, an electron is transferred back from the repaired DNA to FADH° to restore the FADH$^-$.[4] Transient absorption studies, however, argued against the last stage of the mechanism that the FAD remains in the semiquinoid state after repair and may be reduced to FADH$^-$ by a different chemical source.[9]

Since the amino acid sequence of (6−4) photolyase, especially in the FAD binding domain, is similar to that of CPD photolyase, it has been proposed that these two enzymes share a similar structure and reaction scheme.[10−14] However, no crystal structure has been available for (6−4) photolyase, and therefore, its reaction mechanism is not well understood.[15] It has been noted that (6−4) photolyase has a significantly lower quantum yield (0.05−0.1) of DNA repair compared with that of the CPD enzyme (0.7−0.98),[4] and the reason for this remains to be explained.

For a flavin to perform a specific enzymatic reaction, control of its redox potential by a protein is indispensable.[16] To explore the structure of the FAD cofactor and its environment in (6−4) photolyase, we measured resonance Raman spectra of the FAD cofactor in both the neutral semiquinoid and oxidized forms, since resonance Raman spectroscopy is a sensitive tool to probe the structure of flavin and its interactions with the protein environment.[17,18] Normal mode assignments of Raman bands

* Corresponding author. Tel.: +81-564-59-5225. Fax: +81-564-59-5229. Email: teizo@ims.ac.jp.
† Okazaki Institute for Integrative Bioscience.
‡ Graduate University for Advanced Studies.
§ Kyoto University.
|| Present address: Division of Chemistry, Graduate School of Science, Hokkaido University, Sapporo, 060-0810, Japan.
⊥ Present address: Department of Chemistry, Stanford University, 333 Campus Drive, Stanford, California 94305-5080.
⊽ Present address: Toyota Physical & Chemical Research Institute, Nagakute, Aichi. 480-1192, Japan.

Structure and Environment of FAD in (6−4) Photolyase

J. Phys. Chem. B, Vol. 110, No. 33, 2006 **16725**

for the neutral semiquinoid flavin were performed for the first time using density functional theory (DFT) calculations on lumiflavin at the B3LYP/6-31G(d) level. Our results suggest that the FAD of (6−4) photolyase has a structure in which electron density is lacking in the benzene ring and strong hydrogen bonds are formed at N5−H and N1 in an overall hydrophobic environment, and its relationship to functions will be discussed.

Experimental Methods

Enzyme Preparation. The gene of (6−4) photolyase from *Arabidopsis thaliana*[19] was inserted at the *NdeI/SacI* sites of the pET-28a expression vector (Novagen). *Escherichia coli* BL21(DE3) transformed with the vector was inoculated into 0.5 L of culture in a 3-L flask and grown at 37 °C in LB medium to OD_{600} of 1.5 and then cooled to 26 °C. IPTG was added to 0.2 mM. The culture was further incubated for about 24 h and then harvested. After harvest, the pellet was frozen at −80 °C, thawed, and resuspended in a lysis buffer (20 mM sodium phosphate, 0.5 M NaCl, 1 mM DTT, 5% glycerol, pH 7.4). Following the sonication, the cell debris was removed by ultracentrifugation. The cell-free extract was loaded onto a HisTrap HP column (Amersham), and the fusion protein was eluted with the elution buffer (20 mM sodium phosphate, 0.5 M NaCl, 0.5 M imidazole, pH 7.4). Then, the sample was applied to a HiTrap Heparin HP column (Amersham) and eluted with a linear gradient of NaCl from 0.3 to 1 M. The sample was identified as a monomeric form by a HiLoad 16/60 Superdex 200 prep grade column (Amersham). Starting from 2 L of the *E. coli* culture, ca. 12 mg of the purified protein was obtained after the Heparin column.

The purified enzyme was stored in 20 mM sodium phosphate (pH 7.4) containing 0.5 M NaCl. Purity of the protein after the Heparin column was determined by SDS−PAGE, and the molecular weight of the monomeric enzyme was confirmed with the gel filtration method under the assumption that the elution volume of the Superdex 200 column was the same as that scaled by Gel Filtration Calibration Kit (Amersham). The concentration of the oxidized form of the enzyme was estimated on the basis of the FAD absorbance at 450 nm ($\epsilon_{450} = 1.12 \times 10^4$ M^{-1} cm^{-1}),[20] and that of the neutral semiquinoid form was estimated from the absorbance at 580 nm ($\epsilon_{580} = 4.8 \times 10^3$ M^{-1} cm^{-1}).[21]

Enzyme Photoreduction. (6−4) Photolyase as purified is composed of semiquinoid FAD and oxidized FAD. All the semiquinoid enzymes in this mixture were completely oxidized by air in 48 h because of its sensitivity to oxygen. To prepare the semiquinoid form, the oxidized enzyme was photoreduced by laser irradiation at 442 nm from a He−Cd laser (Kimmon Electric, IK4101R−F). First, 100 μL of the solution containing 150 μM (6−4) photolyase was placed in a cylindrical Raman cell and sealed with a rubber septum. Then, the inside of the cell was replaced with N$_2$, and the cell was spun at a rate of 2000 rpm. The laser light was focused onto the sample evenly with a quartz lens of 150-mm focal length to increase the efficiency of photoreduction. To avoid the cell heating by laser illumination, the spinning cell was cooled by flushing with cold N$_2$ gas passed through liquid N$_2$. About 30 min illumination with 30 mW laser light was sufficient to reduce 150 μM (6−4) photolyase. Reduction of a majority of the oxidized FAD to the semiquinoid form was confirmed with absorption spectra.

Enzyme Activity. The method for measuring the enzyme activity of (6−4) photolyase was based on the procedure established for CPD photolyase.[22] A substrate of the damaged DNA was prepared through irradiation of p(dT)$_8$ by 254 nm

UV light from a UV transilluminator (Vilber Lourmat, TFX-20-MC) with 6.4 mW/cm^2 of intensity for 30 min using the cylindrical spinning cell cooled by cold N$_2$. The complex of 2 μM (6−4) photolyase with 50 μM damaged p(dT)$_8$ in 50 mM Tris-HCl (pH 7.4), 200 mM NaCl, and 1 mM DTT was illuminated by tungsten light (Sigma Koki, PHL-150) at room temperature. The UV−vis absorption spectrum of the reacting sample in the spinning cell was measured at 1-min intervals.

Absorption and Resonance Raman Spectroscopy. Optical absorption spectra of samples were recorded with a Hitachi UV-3310 UV−vis spectrophotometer at room temperature. Resonance Raman spectra were obtained with a single monochromator (Jobin Yvon, SPEX750M) equipped with a liquid N$_2$-cooled CCD detector (Roper Scientific, Spec10:400B/LN). The excitation wavelengths used were 568.2 and 488.0 nm from a krypton−argon mixed gas ion laser (Spectra Physics, BeamLok 2060) for the semiquinoid and oxidized forms, respectively. The laser power at the sample point was 5 mW. Rayleigh scattering was removed with appropriate holographic notch filters (Kaiser Optical Systems). Raman shifts were calibrated with indene, and the accuracy of the peak positions of the well-defined Raman bands was ±1 cm^{-1}.

An aliquot of the 150 μM enzyme solution in 20 mM sodium phosphate buffer at pH 7.4 containing 0.5 M NaCl was used for the measurement of the semiquinoid form, while the 80 μM enzyme or isolated FAD solution in the same buffer was used for the measurements of the oxidized enzyme or isolated FAD. All the measurements were performed with a spinning Raman cell containing 100 μL of the sample solution, and the semiquinoid samples were purged with N$_2$ to avoid the oxidation. All samples were cooled with cold N$_2$ gas. The structureless background in the final spectrum was removed by a polynomial subtraction procedure by *Igor Pro 5.03* (Wave-Metrics).

Density Functional Theory Calculations. To analyze the Raman bands of the FAD neutral semiquinoid form, geometry optimizations and frequency calculations were carried out for a model compound, lumiflavin, in its neutral radical semiquinoid form by the DFT method on the B3LYP/6-31G(d) level. To see the deuterated effect of flavin on calculated normal modes and those frequencies, the H atom bound at the N3 and N5 positions was replaced with the D atom. The structures with the minimal energy were confirmed by the absence of imaginary frequencies. The obtained frequencies were scaled by the widely accepted single scaling factor of 0.9614.[23] All calculations were carried out on an SGI2800 high-performance computer (Research Center for Computational Science, Okazaki) using the program package *Gaussian 03*.[24]

Results

Enzyme Activity of (6−4) Photolyase. Figure 1 shows the time course of dimer repair observed with 2 μM (6−4) photolyase and 50 μM damaged p(dT)$_8$ in the reaction buffer as described in the Experimental Methods. For the damaged DNA, the 266 nm band of normal DNA is decreased significantly, and a band at 325 nm of the (6−4) photoproducts[25] is appreciable. Along the illumination of white light for the damaged DNA in the presence of (6−4) photolyase, reappearance of the band at 266 nm (a) and disappearance of the band at 325 nm (b) were observed, while no change was observed in the absence of the enzyme (data not shown), demonstrating that the His-tagged enzyme used in this study is active like a GST-tagged enzyme.[19]

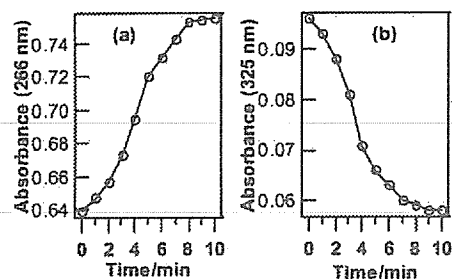**Absorption Spectra of (6−4) Photolyase.** The three redox states including oxidized (FAD_{ox}), semiquinoid (FADH°), and

Figure 1. Effect of illumination time on the extent of dimer repair by the His-tagged enzyme used in this experiment observed with damaged p(dT)$_8$. Absorbance at 266 nm (a) and that at 325 nm (b) of (6—4) photoproducts are plotted against time.
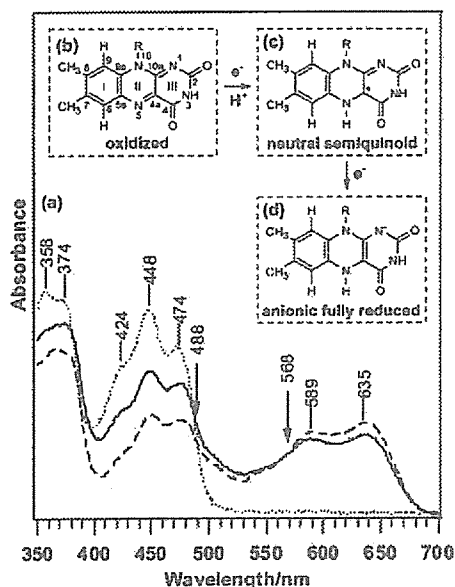

Figure 2. Absorption spectra of (6—4) photolyase from *Arabidopsis thaliana* (a) and the structure and atomic numbering schemes of flavin in three redox states (b—d). For (a), the solid line shows the spectrum of the enzyme immediately after purification, which is a mixture of a neutral semiquinoid form and an oxidized form, the dashed line shows the photoreduced enzyme with a majority amount of the neutral semiquinoid form, and the dotted line shows that of the fully oxidized form. The arrows indicate the Raman excitation wavelengths. (b) Oxidized form. (c) Neutral semiquinoid form. (d) Anionic fully reduced form.

Figure 3. Resonance Raman spectra of (6—4) photolyase from *Arabidopsis thaliana* which was photoreduced by blue light in H$_2$O (A), immediately after purification in H$_2$O (B) and in D$_2$O (C). Spectrum (D) was observed after 10 min in the repeated measurement in D$_2$O. Spectrum (E) were observed for the enzyme which was oxidized completely first and photoreduced subsequently by blue light in D$_2$O. The Raman excitation wavelength was 568.2 nm.

fully reduced (FADH$^-$) forms, are possible for an isoalloxazine ring, and their structures and atomic numbering are illustrated in Figure 2(b—d). Immediately after purification, the enzyme was a mixture of FAD$_{ox}$ and FADH$^\circ$ as shown by a solid line in Figure 2a. The fully oxidized form, which is shown by a dotted line in Figure 2a, was obtained by exposure of the above mixture to air for 48 h. The absorption spectrum of the fully oxidized (6—4) photolyase is remarkably different from that of FAD in a polar solvent, while it is similar to that in a nonpolar solvent.[26] The similarity of absorption spectra suggests that FAD in (6—4) photolyase is bound in a less polar environment.

The semiquinoid form was obtained by reduction of the oxidized enzyme by irradiation of blue light as explained in the Experimental Methods, which gave an absorption spectrum as the dashed line in Figure 2a. The absorption maxima at 589 and 635 nm of a solid and dashed line in Figure 2a are due to the π—π* electronic transition of FADH$^\circ$, while they are completely absent in the spectra of FAD$_{ox}$ and FADH$^-$ (data not shown). On account of these absorption spectra, 568.2 nm was chosen as the Raman excitation wavelength to selectively

enhance the neutral semiquinoid form, while 488.0 nm was chosen to enhance the pure oxidized form.

Resonance Raman Spectra of Semiquinoid (6—4) Photolyase. The resonance Raman spectra of the photoreduced form in H$_2$O is shown in Figure 3A. The prominent bands in the H$_2$O solution at 1606, 1522, 1398, 1298, and 1220 cm^{-1} correspond well to bands of riboflavin neutral semiquinoid radical generated by pulse radiolysis at 1617, 1542, 1387, 1296, and 1225 cm^{-1}, which are Raman spectroscopically distinct from those of anion and cation radicals.[27] Therefore, Figure 3A demonstrates the formation of a neutral semiquinone (Figure 2c) in (6—4) photolyase. The spectrum B in Figure 3 is of the enzyme immediately after purification. Although the enzyme contains some amount of the oxidized form as shown in Figure 2a, the observed Raman spectrum (Figure 3B) is almost identical to that of the photoreduced form (Figure 3A), since the bands are solely ascribed to the semiquinoid form due to the advantage of resonance effect of Raman excitation at 568.2 nm.

Spectrum C was observed for the sample whose solvent was replaced with D$_2$O immediately after purification of the enzyme in H$_2$O. Spectrum C is different from spectrum B with regard to the bands at 1341, 1323, and 1227 cm^{-1}, indicating that deuteration occurred. However, prolonged measurements brought about further changes. After 10 min of measurements, for example, the bands at 1522 and 1606 cm^{-1} seemed to split into

TABLE 1: Raman Frequencies (cm⁻¹) of Neutral Radical Semiquinoid Flavins and Flavoproteins[i]

compound	solvent						Raman bands									
[a](6-4) PL, FADH°	H₂O	1606		1522			1398	1374	1338	1330		1298	1279	1220	1198
[a](6-4) PL, FADH°	D₂O	1608	1594	1536	1508	1456	1397			1328		1295		1218	1199
[b]CPD PL, FADH°	H₂O	1607		1529			1392	1378	1347	1332		1303	1260	1222	1198
[b]CPD PL, FADH°	D₂O	1607	1593	1529	1508		1392	1378		1332	1325	1302	1260	1222	
[c]CPD PL, FADH°	H₂O	1606		1528			1391			1332		1301		1220	
[c]CPD PL, FADH°	D₂O	1606	1594	1528			1390	1377		1332	1322	1300		1219	
[d]P-450 Rd, FADH°	H₂O	1611		1540			1378					1305	1264	1226	
[d]P-450 Rd, FMNH°	H₂O	1611		1532			1388					1304	1268	1227	1200
[e]Ad Rd, FADH°	H₂O	1611							1344			1310	1271		
[f]Fd, FMNH°	H₂O	1611		1535			1391	1378	1333	1314		1308	1269	1232	
[g]Fd, FMNH°	D₂O	1611					1386								
[h]riboflavin, RFH°	H₂O	1617		1542			1387					1296		1225	

[a] This work. [b] Ref 29. [c] Ref 28. [d] Ref 32. [e] Ref 31. [f] Refs 32, 48. [g] Ref 48. [h] Ref 27. [i] PL: photolyase. Rd: reductase. Ad: adrenodoxin. Fd: flavodoxin. RF: riboflavin.

three and two bands, respectively, as illustrated in spectrum D. The sample of E was obtained separately by photoreduction in D₂O after complete oxidation of the purified enzyme in air. Because the proton attached at N5 of the semiquinoid flavin is released from the nitrogen atom in the oxidized form (Figure 2b), the above processes of oxidation and subsequent photoreduction in D₂O lead complete replacement of the H atom at N5 with the D atom. Accordingly, the spectral change in spectrum D compared with spectrum C seems to reflect the progress of N5-deuteration of FAD through photoreduction by the probe light along measuring time. Since spectrum C is different from either spectrum B in H₂O or spectrum E of the fully N5—D form, it is considered to reflect the N3—D form. It means that spectra C and E correspond to the N3—D/N5—H and N3—D/N5—D forms of isoalloxazine, respectively. Accordingly, the bands at 1594, 1536, 1508, and 1456 cm⁻¹ are characteristic of N5—D, while those around 1200—1350 cm⁻¹ are mainly due to N3—D.

Raman bands of the FADH° of (6—4) photolyase are listed in Table 1 and are compared with those of other flavins and flavoproteins in a neutral radical form.[27-29,31,32,48] It is noted that the frequencies of prominent Raman bands of (6—4) photolyase are close to those of CPD photolyase. No Raman bands have been found so far in the 1400—1500 cm⁻¹ region for the neutral semiquinoid flavins.[27] For (6—4) photolyase in the N5—D form, however, a band was observed at 1456 cm⁻¹ for the first time. The reported Raman studies on CPD photolyase have not discussed the bands in this region because of the interference by the bands of Hepes[29] or glycerol[28] in the solvent. We can avoid this problem by using 20 mM phosphate buffer without glycerol. Vibrational assignment of these bands will be described quantitatively later on the basis of DFT calculations.

Resonance Raman Spectra of Oxidized (6—4) Photolyase. Figure 4 shows the resonance Raman spectra of the oxidized (6—4) photolyase in H₂O (A) and D₂O (B). The vibrational assignment of the oxidized flavin has been well-established,[33-36] and the customary numbering of Raman bands is given in the upper part of the figure. Band I of the oxidized flavin, which is attributed to an almost pure ring I mode and is generally observed around 1630 cm⁻¹,[32,33,36-45] appeared at a distinctly lower frequency for (6—4) photolyase (1621 cm⁻¹ in both H₂O and D₂O). All bands above 1340 cm⁻¹ are H₂O/D₂O insensitive, meaning that they arise from rings I and/or II, since neither ring has exchangeable protons. However, the bands at 1254, 1266, and 1320 cm⁻¹ in H₂O were shifted to lower or higher frequencies in D₂O (1241 and 1330 cm⁻¹). These are characteristic of the C2—N3 and N3—C4 stretching modes coupled with the N3—H bending mode, which exhibits a higher
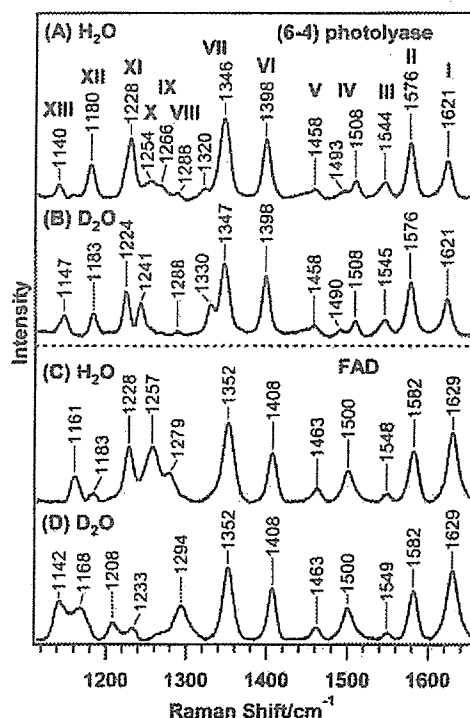
Figure 4. Resonance Raman spectra of oxidized (6—4) photolyase from *Arabidopsis thaliana* in H₂O (A) and D₂O (B) and those of free FAD in H₂O (C) and D₂O (D). The excitation wavelength was 488.0 nm. The FAD solution contains 4 M KI to quench fluorescence. Band numbering is according ref 34.

frequency shift upon removal of the coupling with N—H bending vibration in the N3—D form[38] but is shifted to lower by the coupling with the N3—D bending vibration.

Since the Raman spectrum of the oxidized CPD photolyase has not been reported yet, the spectra of the protein-free FAD in H₂O (C) and D₂O (D), measured under the same experimental condition except for addition of 4 M KI to quench the fluorescence, are presented for comparison in the lower part of Figure 4. The bands above 1350 cm⁻¹ are generally insensitive to the H/D substitution, in agreement with the results of (6—4) photolyase. The bands of free FAD in H₂O in the 1150—1300 cm⁻¹ region are shifted in D₂O in a complicated way, reflecting the participation of the N3—H bending vibration. The differences in these frequencies between (6—4) photolyase and free FAD are caused by differences in H-bonding at N3—H with the protein in water.

From the comparison of rings I and II modes between (6—4) photolyase and free FAD, it is noticed that frequencies are generally lower and the intensity of the band at 1621 cm⁻¹ (band

16728 J. Phys. Chem. B, Vol. 110, No. 33, 2006

Li et al.

TABLE 2: Assignments of Raman Bands of Neutral Radical Semiquinoid Flavin in (6–4) Photolyase

observed (6–4) photolyase				calculated frequencies for lumiflavin[a]			
H2O ν/cm^{-1}	D2O intermediate ν/cm^{-1}	D2O	mode	N3–H N5–H ν/cm^{-1}	N3-D N5–H $\Delta\nu/cm^{-1}$	N3-D N5-D $\Delta\nu/cm^{-1}$	approximate descriptions
1606	1606	1608	ν_{75}	1602	−1	−1	ν (ring I)
		1594	ν_{74}	1591	0	−7	ν (ring I), δ (N5–H), ν (N1=C10a), ν (C4a–N5)
		1536	ν_{73}	1539	0	0	ν (ring I), ν (N1=C10a)
1522	1522	1508	ν_{72}	1503	0	−2	ν (ring I), δ (N5–H)
		1456	ν_{71}	1495	−1	−46	δ (N5–H), ν_{asym} (C4a–N5–C5a), ν (N1=C10a)
1398	1398	1397	ν_{61}	1398	0	−2	ν (ring I), ν (N1=C10a), ν (C4a–N5), ν_{asym} (C9a–N10–C10a)
1338	1330	1328	ν_{59}	1345	−4	−19	δ (N5–H), δ (N3–H), ν_{sym} (C9a–N10–C10a), ν_{sym} (C10a–N1–C2), ν_{asym} (N3–C4–C4a)
1330			ν_{58}	1335	−124	−170	δ (N3–H), δ (N5–H)
1298	1298	1295	ν_{57}	1312	−1	−5	ν (ring I), ν_{sym} (C9a–N10–C10a), δ (N5–H)
1279			ν_{56}	1298	+5	+2	ν (ring I), ν_{asym} (C9a–N10–C10a), δ (N3–H), δ (N5–H)

[a] Calculated using density functional theory (DFT) by *Gaussian 03* with B3LYP/6-31G(d) basis functions.

(A) N3-H/N5-H

(B) N3-D/N5-D

ν_{75} 1602 cm⁻¹ ν_{74} 1591 cm⁻¹ ν_{75} 1601 cm⁻¹ Δv= -1 ν_{74} 1584 cm⁻¹ Δv= -7

ν_{73} 1539 cm⁻¹ ν_{72} 1503 cm⁻¹ ν_{73} 1539 cm⁻¹ Δv= 0 ν_{72} 1501 cm⁻¹ Δv= -2

ν_{71} 1495 cm⁻¹ ν_{61} 1398 cm⁻¹ ν_{65} 1449 cm⁻¹ Δv= -46 ν_{61} 1396 cm⁻¹ Δv= -2

ν_{59} 1345 cm⁻¹ ν_{58} 1335 cm⁻¹ ν_{59} 1326 cm⁻¹ Δv= -19 ν_{52} 1165 cm⁻¹ Δv= -170

ν_{57} 1312 cm⁻¹ ν_{56} 1298 cm⁻¹ ν_{58} 1307 cm⁻¹ Δv= -5 ν_{57} 1300 cm⁻¹ Δv= +2
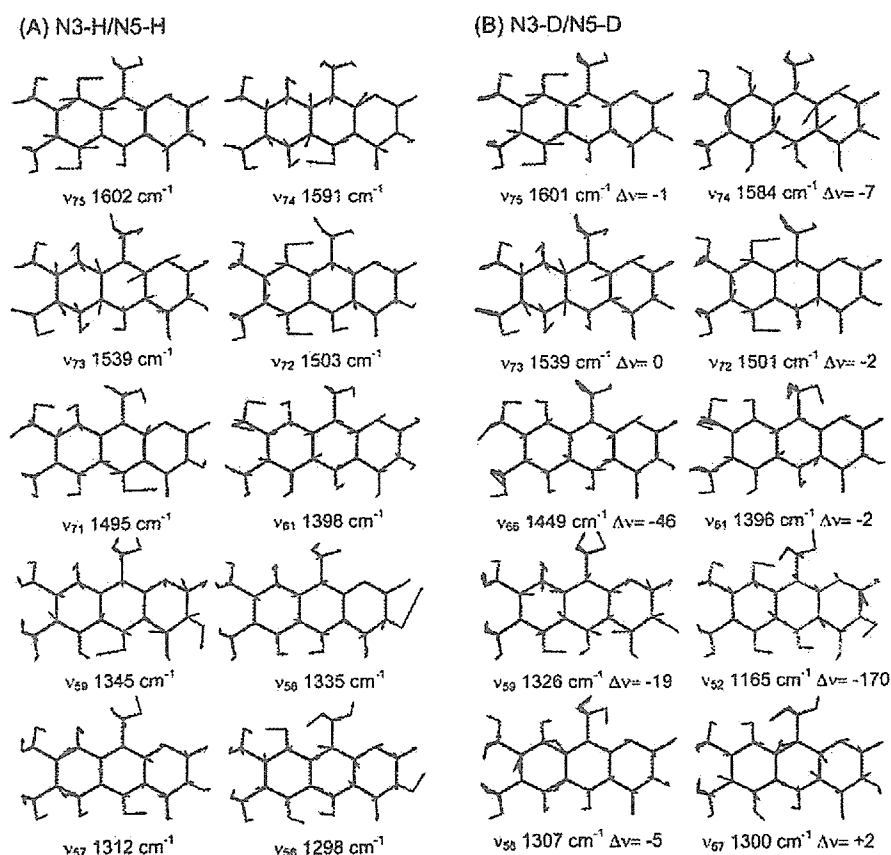
Figure 5. Normal modes of some typical marker bands for neutral radical semiquinoid lumiflavin (A) and its corresponding N3–D/N5–D form (B). Vibrational frequencies and displacements were calculated by DFT method using *Gaussian 03* with B3LYP/6-31G(d) basis functions.

I) is weaker for protein than for free FAD. Since band II is known to exhibit downshifts upon formation of a hydrogen bond at N1,[36] its lower frequency suggests that a strong hydrogen bond is formed at N1 of FAD in (6–4) photolyase. Splittings of band IV (1508 and 1493 cm⁻¹) and band VII (1346 and 1320 cm⁻¹) of the oxidized (6–4) photolyase are used as a marker of "buried" character of the flavin environment.[33] In fact, both bands are observed as a single band for free FAD (spectrum C), while it is split in a solid state.[33] Therefore, this observation indicates that the isoalloxazine ring of (6–4) photolyase is held in a well-formed protein pocket from which water molecules might be excluded. In addition, it is noted that the downshifted and weakened band I (1621 cm⁻¹), intensified band III (1544 cm⁻¹), downshifted band VI (1398 cm⁻¹), downshifted and weakened band IX (1266 cm⁻¹), weakened band X (1254 cm⁻¹), downshifted and intensified band XII (1180 cm⁻¹), and weak-

ened band XIII (1140 cm⁻¹) all resemble the spectral characteristics of flavin placed in a less polar solvent.[40,46]

Density Functional Theory Calculation for Neutral Radical Semiquinoid Lumiflavin. Since there has been no theoretical treatment of vibrational spectra of neutral semiquinone of flavin, we carried out DFT calculations on lumiflavin at B3LYP/6-31G(d) level, and the results are summarized in Table 2, where the frequencies observed for (6–4) photolyase in H2O and D2O are compared with those calculated (scaled by a factor of 0.9614)[23] for the N3–H/N5–H, N3–D/N5–H, and N3–D/N5–D forms. In addition, included are the mode numbers and the approximate descriptions for vibrational character. Calculated vibrational modes are also illustrated in Figure 5, where the displacements of atoms are explicitly represented.[47] Cartesian coordinates of atoms in the minimal potentials obtained are given

Structure and Environment of FAD in (6—4) Photolyase

J. Phys. Chem. B, Vol. 110, No. 33, 2006 **16729**

by Table S1 in the Supporting Information. The mode numbers are assigned tentatively in the order of increasing frequency, although the numbering is not established yet. Tentative assignments of the Raman bands observed for FADH° in (6—4) photolyase are also contained.

According to this calculation, the prominent band at 1606 cm^{-1} in H$_2$O can be assigned to an overlapped band of ν_{75} and ν_{74}, which include ring I and primarily ring II vibrations, respectively. ν_{75} does not shift upon N5—H deuteration, while ν_{74} downshifts by 7 cm^{-1} due to fairly large involvement of N5—H bending motion in the ν_{74} mode. Therefore, they are observed as separate bands in D$_2$O.

The alteration of resonance Raman band in the 1400—1550 cm^{-1} region upon deuterium substitution exhibits complex behavior. The 1522 cm^{-1} band observed in H$_2$O seems to split into 1536, 1508, and 1456 cm^{-1} in D$_2$O, as judged from concomitant intensity decrease of the 1522 cm^{-1} band and intensity increase of those three bands. These bands were presumably assigned to the three computed normal modes, ν_{73}, ν_{72}, and ν_{71}, in the 1500—1540 cm^{-1} region. Upon deuteration, the normal coordinate compositions are altered for the vibrational modes in this region and thereby resonance Raman intensity redistribution, which are interpreted below. The ν_{73} mode is mainly composed of the N1=C10a stretching and ring I symmetric modes and is expected to get strong resonance Raman enhancement due to a large change in polarizability along those symmetric modes. Furthermore, appreciable excited-state distortion of the N$_1$=C$_{10a}$ bond is expected upon the $\pi—\pi^*$ excitation at 568.2 nm, and it would cause redistribution of electron density regarding the N1=C10a bond. The ν_{73} mode does not include vibration arising from N—H motion and thus does not show a large change in both the frequency and the normal mode in the deuterated form. The ν_{72} mode mainly consists of C—H bending in ring I and N—H bending which is coupled weakly with the ring I mode. Upon deuteration, the coupling of the N—H motion is removed, showing a slight downshift in the frequency. The ν_{72} mode in the H-form may not be strongly resonance enhanced due to the C—H bending character of the vibrational mode. However, upon deuteration, the ν_{72} normal mode compositions are slightly altered. As mentioned above, the coupling with N—H bending is removed, and the mixing of the N1=C10a stretching mode could cause resonance enhancement of Raman intensity. The ν_{71} mode at 1495 cm^{-1} is mainly composed of N5—H bending, to which N1=C10a stretching and the asymmetric C4a—N5—C5a stretching [ν_{asym}(C$_{4a}$—N$_5$—C$_{5a}$)] that can be intensity-enhanced by the $\pi—\pi^*$ excitation are coupled. This mode should show a large deuterium isotope shift, and the corresponding mode in the deuterium substituted form could be found as the ν_{66} mode at 1449 cm^{-1}. Thus, the 1456 cm^{-1} band observed in D$_2$O would arise from the ν_{66} mode. In the H$_2$O form, however, the ν_{66} mode is mainly composed of C—H bending motion of the methyl substituents of ring I, which would not gain resonance Raman enhancement. When N5 is deuterated, ν_{66} contains the N1=C10a and C4a—N5 stretchings and accordingly gains Raman intensity.

The intense band of Figure 3A at 1398 cm^{-1} is assignable to ν_{61}, which involves N1=C10a and C4a—N5 stretching. Therefore, its frequency would be insensitive to deuterium exchange as observed both theoretically and experimentally. The shoulder peak at 1391 cm^{-1} and the nearby weak band at 1374 cm^{-1} disappear in D$_2$O. A couple of bands around 1338 cm^{-1} probably arise from ν_{59} and ν_{58}. The ν_{58} mode is almost pure N3—H and N5—H deformational mode, which exhibits a large

downshift in the frequency upon deuteration. The bands of Figure 3A at 1298 and 1279 cm^{-1} are probably assigned to ν_{57} and ν_{56}, respectively.

Discussion

Comparison with CPD Photolyase. The marker band of the neutral semiquinoid flavin[30] for (6—4) photolyase was observed at 1606 cm^{-1} (Figure 3A), which is similar to that observed for CPD photolyase at 1607[29] or 1606[28] cm^{-1} (Table 1). These frequencies are lower than those of other flavins and flavoproteins.[27-32,48,49] However, this marker band at 1606 cm^{-1} in (6—4) photolyase in H$_2$O splits into two comparable bands at 1608 and 1594 cm^{-1} in D$_2$O (Figure 3E), whereas that of CPD photolyase in D$_2$O remains a single band with a shoulder at 1593 cm^{-1}, which is very similar to that of (6—4) photolyase obtained after prolonged measurement in Figure 3D. Figure 3D is inferred to arise from the incompletely N5-deuterated sample, because for (6—4) photolyase, the redox cycle in this study (oxidation and subsequent photoreduction in D$_2$O) enforced the release of the N5 proton of flavin and replaces it with deuterium in a D$_2$O solvent, which gives the spectrum of the completely N5-deuterated sample as observed in Figure 3E. Consequently, it is highly likely that the reported spectrum of CPD photolyase in D$_2$O[28,29] reflects an incompletely N5-deuterated enzyme. The assignment from DFT calculations that ν_{74} is low-frequency shifted but ν_{75} is invariable in the N5—D form (Table 2) also supports that the deuterium exchange at N5 causes its apparent splitting.

Another H/D-sensitive band at 1522 cm^{-1} in H$_2$O splits into three bands at 1456, 1508, and 1536 cm^{-1} in D$_2$O. The split band at 1508 cm^{-1} was observed for CPD photolyase in one report[29] but not in the other,[28] while the split band at 1456 cm^{-1} has not been observed in flavoproteins before. This apparent splitting is actually a frequency separation of accidentally degenerate bands due to a low-frequency shift of ν_{72} and ν_{71} in D$_2$O, while the higher-frequency counterpart (ν_{73}) is less sensitive to N5 deuteration. Although the corresponding Raman band of CPD photolyase at 1528[28] or 1529[29] cm^{-1} had no H/D effect, a similar H/D-sensitive resonance Raman band in this region was also observed for *Clostridium Mp*. Flavodoxin.[48]

A prominent H/D-insensitive band was observed at 1398 cm^{-1} (with a shoulder at 1391 cm^{-1}) and a nearby H/D-sensitive band at 1374 cm^{-1}. The corresponding bands in CPD photolyase were observed at 1392 and 1378 cm^{-1}, respectively. Schelvis et al. proposed that the band at 1378 cm^{-1} in CPD photolyase might be a marker for the MTHF or its structural role by stabilizing the protein environment of the FAD cofactor,[29] because this band was not observed for the MTHF-free mutant of CPD photolyase.[28] Since the purified (6—4) photolyase in this study does not contain the second chromophore, the 1374 cm^{-1} band cannot be ascribed to the MTHF moiety. Our theoretical assignment suggests that the intense band at 1398 cm^{-1} arises from the ν_{61} mode. Since ν_{61} involves N1=C10a and ring II stretching characters, its strong resonance Raman intensity is reasonable. The weak band at 1374 cm^{-1} probably arises from ring III of FAD in H$_2$O but is shifted to lower frequencies upon N3 deuteration.

H-bonding Environment of FAD in (6—4) Photolyase. The crystal structure of *E. coli* CPD photolyase revealed the H-bonding environment of FAD as illustrated in Figure 6. Hydrogen bonds are formed at N1, N3—H, C4=O, and N5—H in CPD photolyase. The 2'-OH of the ribityl chain forms a hydrogen bond with N1 probably because of the unusual U-shaped FAD structure. N3—H donates a hydrogen bond to

(A)

FAD

Asp372

Asn378

Asp374

(B)

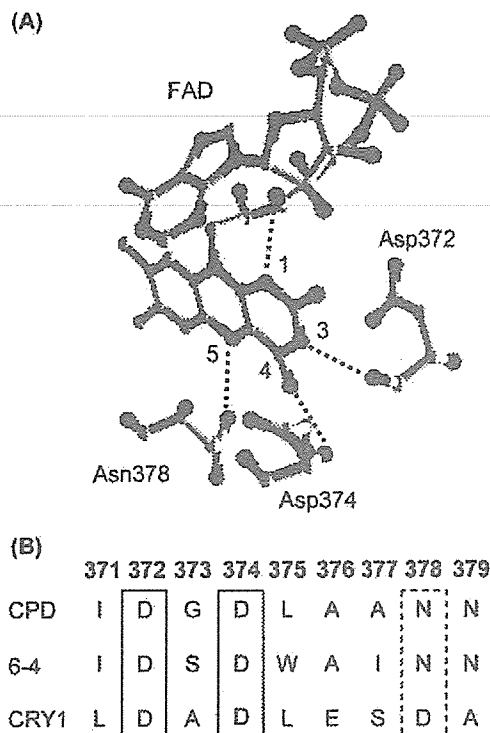|	371	372	373	374	375	376	377	378	379
CPD	I	D	G	D	L	A	A	N	N
6-4	I	D	S	D	W	A	I	N	N
CRY1	L	D	A	D	L	E	S	D	A

Figure 6. Structure and sequence alignment for flavin center. (A) Crystal structure of *E. coli* CPD photolyase. (B) Alignment of *E. coli* CPD photolyase, *Arabidopsis thaliana* (6—4) photolyase, and *Arabidopsis thaliana* cryptochrome 1 over the region in H-bonding distance from isoalloxazine (from refs 5, 19, 50).

Asp372 (numbering in *E. coli* CPD photolyase), C4=O accepts a hydrogen bond from Asp374, and N5—H donates a hydrogen bond to Asn378. These amino acids involving hydrogen bonds are conserved in (6—4) photolyase. A very similar U-shaped FAD and H-bonding environment were also observed for the structure of the photolyase-like domain of cryptochrome 1 from *Arabidopsis thaliana*, except that the Asn378, which is contacted with N5—H, is replaced by Asp.[50] A sequence alignment in this region is illustrated in Figure 6B. From the sequence alignment and resonance Raman spectra of (6—4) photolyase, the presence of similar hydrogen bonds at N5—H and N1 in (6—4) photolyase is indicated as discussed below.

We have already pointed out that the 1606 cm^{-1} marker band is assignable to an overlapped band of ν_{74} and ν_{75}. Its significantly lower frequency is a common feature to photolyases: 1607 cm^{-1} for CPD photolyase and 1606 cm^{-1} for (6—4) photolyase. Murgida et al. attributed the origin of the unusually low frequency of this band to a stronger hydrogen bond at N5—H,[28] although Schelvis et al. argued against it, because its frequency is rather insensitive to H/D exchange. However, as mentioned above, deuteration in the sample of Schelvis et al. was probably incomplete, and presumably, N5—H was not replaced with deuterium. In this study, splitting of this marker band into two comparable components at 1608 and 1594 cm^{-1} was observed for the completely deuterated FAD cofactor in Figure 3E. The normal modes of ν_{74} assigned for 1594 cm^{-1} band involve N5—H bending deformations (Table 2, Figure 5), which will downshift upon H-bonding at N5—H as discussed by Murgida et al. before.[28] Therefore, the unusually low frequency of this marker band would indicate a strong hydrogen bond at N5—H in both the photolyases. Similarly, the lower frequencies of the 1522 cm^{-1} band in (6—4) photolyase and 1529 cm^{-1} band in CPD photolyase, which are presumably assigned to the modes of ν_{73}—ν_{71} with N5—H bending in ν_{72}

and ν_{71}, also indicate a strong hydrogen bond at N5—H. This band was empirically used as an indicator of a hydrogen bond at N5—H in the Raman study on P-450 reductase,[32] and it is justified by this study. Furthermore, judging from the lower frequencies of 1606 and 1522 cm^{-1} in (6—4) photolyase, the N5—H hydrogen bond would be much stronger in (6—4) photolyase than that in CPD photolyase.

As mentioned above, band II of the oxidized (6—4) photolyase indicates a strong hydrogen bond at N1. This hydrogen bond would be caused by the U-shaped FAD conformation as shown in Figure 6. The proteins in this family are believed to be characterized as the unique U-shaped FAD in which an adenine ring approaches the isoalloxazine ring near the N10—C10a moiety, whose stretching significantly contributes to the ν_{61} mode of the semiquinoid form (Table 2). Therefore, the ring stacking geometry may affect the ν_{61} Raman frequency and intensity and may cause the appearance of a weak sideband at 1391 cm^{-1} in Figure 3A. The coupled bands around 1338 cm^{-1}, which involve N3—H and N5—H bending, have a different frequency (1325 cm^{-1}) and profile from that in CPD photolyase which may indicate different H-bonding environments between these two enzymes. On all accounts, the hydrogen bonds predicted for (6—4) photolyase are similar to those of CPD photolyase and cryptochrome except a stronger interaction at N5—H, indicating a similar H-bonding environment of the flavin moiety in the DNA photolyases and blue light photoreceptor family.

Hydrophobic Environment of FAD in (6—4) Photolyase. Resonance Raman and UV—vis absorption spectra of the oxidized FAD in (6—4) photolyase are similar to those of the isolated flavin in a nonpolar solvent. Furthermore, Raman marker bands of "buried" flavin are also observed for (6—4) photolyase. This evidence indicates that the FAD cofactor in (6—4) photolyase is placed in a hydrophobic and less polar environment, as identified for CPD photolyase.[51,52] Spiro's model of flavin, supported by resonance Raman[46] and NMR[53] investigations, argued that the isoalloxazine ring prefers a zwitterionic resonance form in a polar solvent, which results in a higher frequency of band I for the oxidized flavin.[34] According to this model, the observed lower frequency of band I for (6—4) photolyase means a decreased polarity in a flavin pocket.

The hydrophobic environment around FAD of (6—4) photolyase was also suggested by the insensitivity of N5—H to the H/D exchange. To exchange the labile proton with solvent, water molecules must access to the exchange site. The strong hydrophobic environment in the active site of photolyase limits the approach of solvent water to N5 of the flavin ring, which also leads to difficulty in the exchange of N5—H. This coincides with the unexpected finding that N5—H deuteration proceeds little for CPD photolyase as well as (6—4) photolyase.

Low Electron Density of Ring I of FAD in (6—4) Photolyase. Previous work has shown that the C8—Cl substitution of a riboflavin binding protein exhibits a downshift of band I of the oxidized flavin ring I mode from 1631 to 1624 cm^{-1} and weakened it greatly.[54] It is believed that the C8—Cl substitution reduces the electron density of ring I due to the electron withdrawing effect of chloride. Therefore, a significantly low-frequency and weak Raman intensity of band I (1621 cm^{-1}) observed for the oxidized (6—4) photolyase (Figure 4A) suggests that ring I of the oxidized FAD lacks electrons.

The prominent band at 1398 cm^{-1} of FADH° in (6—4) photolyase has a higher frequency than those of other flavins and flavoproteins. This is assignable to ν_{61}, which is an out-of-phase mode of the N1=C10—C4a—N5 stretching and ac-

Structure and Environment of FAD in (6—4) Photolyase

J. Phys. Chem. B, Vol. 110, No. 33, 2006 **16731**

cordingly sensitive to the radical character (Table 2, Figure 5). This assignment is consistent with the intensity loss of the corresponding 1391 cm^{-1} band in CPD photolyase reconstituted with 1,3,5,10-^{15}N—FAD.[28] Thus, its high frequency of 1398 cm^{-1} for (6—4) photolyase and 1391—1392 cm^{-1} for CPD photolyase may mean the higher radical density in the N1= C10a—C4a—N5 moiety. This is consistent with theoretical and EPR studies, which pointed out that FADH° has a more localized radical spin density in CPD photolyase than in other flavoproteins and a very low electron density on ring I.[52,55] This trend is slightly stronger in (6—4) photolyase than in CPD photolyase.

One of the controlling factors of the electron density of flavin is an electrostatic effect.[16] In this family of proteins, two aspartic acids (Asp372 and Asp374, numbering in *E. coli* CPD photolyase) near ring III are conserved. These negatively charged groups would readily induce an electronic perturbation to the ring system, especially to suppress the negative charge of ring III in the resonance form. Thus, the electrostatic effect from the Asp residues may contribute to keep the flavin in photolyases in the neutral form and to make an electron density of ring I low.

Biological Implication. H-bonding environment is an important factor to control the redox states of flavin in flavoproteins.[16] In the study on the control of redox potentials in flavodoxin from Ludwig et al., the G57T mutant, whose hydrogen bond at N5—H of flavin is expected to be weaker evaluated by crystal structure and pK_a of N5—H, has a significantly increased redox potential for the semiquinone/hydroquinone couple.[56] Therefore, an increased H-bonding interaction at N5—H may decrease the redox potential of semiquinoid flavin and make its reduction less favorable. In photolyases, FADH° is generated during repair and must be reduced to FADH$^-$ before the next catalytic cycle. As for CPD photolyase, the FADH° was believed to be reduced by an electron from the repaired DNA, because the quantum yield of this enzyme is almost 1.[4] In our study, (6—4) photolyase has a similar protein environment of FAD cofactor compared with that of CPD photolyase except for a stronger hydrogen bond at N5—H. Therefore, this stronger hydrogen bond may decrease the redox potential of FADH° and make its reduction reaction before the next repair cycle difficult. If the FADH° in (6—4) photolyase is not reduced by repaired DNA but reduced by photoreduction from another photon, the significantly low quantum yield for this enzyme compared with CPD photolyase can be explained.

The hydrophobic and less polar environment, with small reorganization energy, will slow the back electron transfer from substrate radical to neutral semiquinoid FAD before repairing and therefore would be advantageous to electron transfer in the repairing process as pointed out for CPD photolyase.[52,57] Such a scheme will also satisfy the repairing process of (6—4) photolyase, in which a hydrophobic environment of FAD cofactor was revealed.

Although the crystal structures of CPD photolyase showed that ring I is in the direction of the DNA lesion,[5-8] the low spin density and possible low whole electron density on ring I implies that electron transfer between the isoalloxazine ring and CPD would not be direct.[15,55] It was assumed that the adenine of the U-shaped FAD bridges the gap and provides effective coupling between isoalloxazine and damaged DNA.[58,59] On the other hand, the recent study with femtosecond absorption spectroscopy concluded a direct electron jump from the FAD to the CPD, because the intramolecular electron transfer could

not be observed without substrate.[60] In (6—4) photolyase, however, a FAD cofactor with more localized spin density and moderately low electron density of ring I was observed, suggesting a higher possibility of an indirect electron transfer.

Conclusions

The resonance Raman spectra of neutral semiquinoid and oxidized forms of (6—4) photolyase were reported and interpreted with DFT calculations for the first time. The DFT calculations gave a theoretical basis for the behavior of some maker bands in relation with the environment around FAD. It is demonstrated that N5—H of the FAD cofactor of (6—4) photolyase is in a hydrophobic interior and has strong H-bonding interactions with the protein, which explains its peculiar behavior in the H/D exchange as well as the low quantum yield. The unique character of Raman spectra of the oxidized form can also be interpreted in terms of electrostatic and H-bonding interactions of FAD with protein residues conserved in this family of proteins. Implications from this study will be also helpful to understand a mechanism of blue light sensor proteins such as crytochrome 1.

Supporting Information Available: Cartesian coordinates of all calculated models. This material is available free of charge via the Internet at http://pubs.acs.org.

References and Notes

(1) Lindahl, T. *Nature (London)* 1993, *362*, 709—715.

(2) Sancar, A. *Biochemistry* 1994, *33*, 2—9.

(3) Todo, T.; Takemori, H.; Ryo. H.; Ihara, M.; Matsunaga, T.; Nikaido, O.; Sato, K.; Nomura, T. *Nature (London)* 1993, *361*, 371—374.

(4) Sancar, A. *Chem. Rev.* 2003, *103*, 2203—2237.

(5) Park, H. W.; Kim, S. T.; Sancar, A.; Deisenhofer, J. *Science* 1995, *268*, 1866—1872.

(6) Tamada, T.; Kitadokoro, K.; Higuchi, Y.; Inaka, K.; Yasui, A.; de Ruiter, P. E.; Eker, A. P.; Miki, K. *Nat. Struct. Biol.* 1997, *4*, 887—891.

(7) Komori, H.; Masui, R.; Kuramitsu, S.; Yokoyama, S.; Shibata, T.; Inoue, Y.; Miki, K. *Proc. Natl. Acad. Sci. U.S.A.* 2001, *98*, 13560—13565.

(8) Mees, A.; Klar, T.; Gnau, P.; Hennecke, U.; Eker, A. P. M.; Carell, T.; Essen, L. O. *Science* 2004, *306*, 1789—1793.

(9) MacFarlane, A. W.; Stanley, R. J. *Biochemistry* 2003, *42*, 8558—8568.

(10) Todo, T. *Mutat. Res.* 1999, *434*, 89—97.

(11) Todo, T.; Ryo, H.; Yamamoto, K.; Toh, H.; Inui, T.; Ayaki, H.; Nomura, T.; Ikenaga, M. *Science* 1996, *272*, 109—112.

(12) Zhao, X.; Liu, J.; Hsu, D. S.; Zhao, S.; Taylor, J. S.; Sancar, A. *J. Biol. Chem.* 1997, *272*, 32580—32590.

(13) Sancar, A. *Science* 1996, *272*, 48—49.

(14) Kim, S. T.; Malhotra, K.; Smith, C. A.; Taylor, J. S.; Sancar, A. *J. Biol. Chem.* 1994, *269*, 8535—8540.

(15) Weber, S. *Biochim. Biophys. Acta* 2005, *1707*, 1—23.

(16) Miura, R. *Chem. Rec.* 2001, *1*, 183—194.

(17) Morris, M. D.; Bienstock, R. J. *Advances in Spectroscopy*: Clark, R. J. H., Hester, R. E., Eds.; Wiley: New York, 1986; Vol. 13.

(18) Mcfarland, J. T. *Biological Applications of Raman Spectroscopy*; Spiro, T. G., Ed.; Wiley: New York, 1987; Vol. 2.

(19) Nakajima, S.; Sugiyama, M.; Iwai, S.; Hitomi, K.; Otoshi, E.; Kim, S. T.; Jiang, C. Z.; Todo, T.; Britt, A. B.; Yamamoto, K. *Nucleic Acids Res.* 1998, *26*, 638—644.

(20) Todo, T.; Kim, S. T.; Hitomi, K.; Otoshi, E.; Inui, T.; Morioka, H.; Kobayashi, H.; Ohtsuka, E.; Toh, H.; Ikenaga, M. *Nucleic Acids Res.* 1997, *25*, 764—768.

(21) Wang, B. Y.; Jorns, M. S. *Biochemistry* 1989, *28*, 1148—1152.

(22) Jorns, M. S.; Sancar, G. B.; Sancar, A. *Biochemistry* 1985, *24*, 1856—1861.

(23) Scott, A. P.; Radom, L. *J. Phys. Chem.* 1996, *100*, 16502—16513.

(24) Frisch, M. J.; Trucks, G. W.; Schlegel, H. B.; Scuseria, G. E.; Robb, M. A.; Cheeseman, J. R.; Montgomery, J. A., Jr.; Vreven, T.; Kudin, K. N.; Burant, J. C.; Millam, J. M.; Iyengar, S. S.; Tomasi, J.; Barone, V.; Mennucci, B.; Cossi, M.; Scalmani, G.; Rega, N.; Petersson, G. A.; Nakatsuji, H.; Hada, M.; Ehara, M.; Toyota, K.; Fukuda, R.; Hasegawa, J.; Ishida, M.; Nakajima, T.; Honda, Y.; Kitao, O.; Nakai, H.; Klene, M.; Li, X.; Knox, J. E.; Hratchian, H. P.; Cross, J. B.; Bakken, V.; Adamo, C.; Jaramillo, J.; Gomperts, R.; Stratmann, R. E.; Yazyev, O.; Austin, A. J.; Cammi, R.; Pomelli, C.; Ochterski, J. W.; Ayala, P. Y.; Morokuma, K.; Voth, G. A.; Salvador, P.; Dannenberg, J. J.; Zakrzewski, V. G.; Dapprich, S.; Daniels, A. D.; Strain, M. C.; Farkas, O.; Malick, D. K.; Rabuck, A. D.; Raghavachari, K.; Foresman, J. B.; Ortiz, J. V.; Cui, Q.; Baboul, A. G.; Clifford, S.; Cioslowski, J.; Stefanov, B. B.; Liu, G.; Liashenko, A.; Piskorz, P.; Komaromi, I.; Martin, R. L.; Fox, D. J.; Keith, T.; Al-Laham, M. A.; Peng, C. Y.; Nanayakkara, A.; Challacombe, M.; Gill, P. M. W.; Johnson, B.; Chen, W.; Wong, M. W.; Gonzalez, C.; Pople, J. A. *Gaussian 03*, revision C.02; Gaussian, Inc.: Wallingford, CT, 2004.

(25) Franklin, W. A.; Lo, K. M.; Haseltine, W. A. *J. Biol. Chem.* **1982**, *257*, 13535−13543.

(26) Kotaki, A.; Naoi, M.; Yagi, K. *J. Biochem.* **1970**, *68*, 287−292.

(27) Su, Y.; Tripathi, G. N. R. *J. Am. Chem. Soc.* **1994**, *116*, 4405−4407.

(28) Murgida, D. H.; Schleicher, E.; Bacher, A.; Richter, G.; Hildebrandt, P. *J. Raman Spectrosc.* **2001**, *32*, 551−556.

(29) Schelvis, J. P. M.; Ramsey, M.; Sokolova, O.; Tavares, C.; Cecala, C.; Connell, K.; Wagner, S.; Gindt, Y. M. *J. Phys. Chem. B* **2003**, *107*, 12352−12362.

(30) Nishina, Y.; Shiga, K.; Horiike, K.; Tojo, H.; Kasai, S.; Matsui, K.; Watari, H.; Yamano, T. *J. Biochem.* **1980**, *88*, 411−416.

(31) Kitagawa, T.; Sakamoto, H.; Sugiyama, T.; Yamano, T. *J. Biol. Chem.* **1982**, *257*, 2075−2080.

(32) Sugiyama, T.; Nisimoto, Y.; Mason, H. S.; Loehr, T. M. *Biochemistry* **1985**, *24*, 3012−3019.

(33) Zheng, Y. G.; Dong, J.; Palfey, B. A.; Carey, P. R. *Biochemistry* **1999**, *38*, 16727−16732.

(34) Bowman, W. D.; Spiro, T. G. *Biochemistry* **1981**, *20*, 3313−3318.

(35) Abe, M.; Kyogoku, Y. *Spectrochim. Acta, Part A* **1987**, *43*, 1027−1037.

(36) Lively, C. R.; Mcfarland, J. T. *J. Phys. Chem.* **1990**, *94*, 3980−3994.

(37) Dutta, P. K.; Nestor, J. R.; Spiro, T. G. *Proc. Natl. Acad. Sci. U.S.A.* **1977**, *74*, 4146−4149.

(38) Kitagawa, T.; Nishina, Y.; Kyogoku, Y.; Yamano, T.; Ohishi, N.; Takaisuzuki, A.; Yagi, K. *Biochemistry* **1979**, *18*, 1804−1808.

(39) Kitagawa, T.; Fukumori, Y.; Yamanaka, T. *Biochemistry* **1980**, *19*, 5721−5729.

(40) Schmidt, J.; Coudron, P.; Thompson, A. W.; Watters, K. L.; McFarland, J. T. *Biochemistry* **1983**, *22*, 76−84.

(41) Visser, A. J. W. G.; Vervoort, J.; Okane, D. J.; Lee, J.; Carreira, L. A. *Eur. J. Biochem.* **1983**, *131*, 639−645.

(42) Bienstock, R. J.; Schopfer, L. M.; Morris, M. D. *J. Raman Spectrosc.* **1987**, *18*, 241−245.

(43) Desbois, A.; Tegoni, M.; Gervais, M.; Lutz, M. *Biochemistry* **1989**, *28*, 8011−8022.

(44) Tegoni, M.; Gervais, M.; Desbois, A. *Biochemistry* **1997**, *36*, 8932−8946.

(45) Picaud, T.; Desbois, A. *J. Biol. Chem.* **2002**, *277*, 31715−31721.

(46) Muller, F.; Vervoort, J.; Lee, J.; Horowitz, M.; Carreira, L. A. *J. Raman Spectrosc.* **1983**, *14*, 106−117.

(47) Flukiger, P.; Luthi, H. P.; Portmann, S.; Weber, J. *MOLEKEL 4.0*; Swiss Center for Scientific Computing: Manno, Switzerland, 2000.

(48) Dutta, P. K.; Spiro, T. G. *Biochemistry* **1980**, *19*, 1590−1593.

(49) Sakai, M.; Takahashi, H. *J. Mol. Struct.* **1996**, *379*, 9−18.

(50) Brautigam, C. A.; Smith, B. S.; Ma, Z. Q.; Palnitkar, M.; Tomchick, D. R.; Machius, M.; Deisenhofer, J. *Proc. Natl. Acad. Sci. U.S.A.* **2004**, *101*, 12142−12147.

(51) Payne, G.; Wills, M.; Walsh, C.; Sancar, A. *Biochemistry* **1990**, *29*, 5706−5711.

(52) Weber, S.; Mobius, K.; Richter, G.; Kay, C. W. M. *J. Am. Chem. Soc.* **2001**, *123*, 3790−3798.

(53) Vanschagen, C. G.; Muller, F. *Eur. J. Biochem.* **1981**, *120*, 33−39.

(54) Nishina, Y.; Shiga, K.; Horiike, K.; Tojo, H.; Kasai, S.; Yanase, K.; Matsui, K.; Watari, H.; Yamano, T. *J. Biochem.* **1980**, *88*, 403−409.

(55) Kay, C. W. M.; Feicht, R.; Schulz, K.; Sadewater, P.; Sancar, A.; Bacher, A.; Mobius, K.; Richter, G.; Weber, S. *Biochemistry* **1999**, *38*, 16740−16748.

(56) Ludwig, M. L.; Pattridge, K. A.; Metzger, A. L.; Dixon, M. M.; Eren, M.; Feng, Y. C.; Swenson, R. P. *Biochemistry* **1997**, *36*, 1259−1280.

(57) Heelis, P. F.; Hartman, R. F.; Rose, S. D. *Chem. Soc. Rev.* **1995**, *24*, 289−297.

(58) Antony, J.; Medvedev, D. M.; Stuchebrukhov, A. A. *J. Am. Chem. Soc.* **2000**, *122*, 1057−1065.

(59) Medvedev, D.; Stuchebrukhov, A. A. *J. Theor. Biol.* **2001**, *210*, 237−248.

(60) Kao, Y. T.; Saxena, C.; Wang, L. J.; Sancar, A.; Zhong, D. P. *Proc. Natl. Acad. Sci. U.S.A.* **2005**, *102*, 16128−16132.

Photoreaction Cycle of the Light, Oxygen, and Voltage Domain in FKF1 Determined by Low-Temperature Absorption Spectroscopy[†]

Kazunori Zikihara,[‡,§] Tatsuya Iwata,[ǁ] Daisuke Matsuoka,[‡] Hideki Kandori,[ǁ] Takeshi Todo,[§] and Satoru Tokutomi*,[‡]

Department of Biological Science, Graduate School of Science, Osaka Prefecture University, 1-1 Gakuencho, Sakai, Osaka 599-8531, Japan, Department of Material Science and Engineering, Nagoya Institute of Technology, Showa-ku, Nagoya 466-8555, Japan, and Radiation Biology Center, Graduate School of Medicine, Kyoto University, Yoshidakonoe-cho, Sakyo-ku, Kyoto 606-8501, Japan

ABSTRACT: Flavin-binding Kelch repeat F-box (FKF1) protein plays important roles in the photoregulation of flowering in *Arabidopsis*. FKF1 has a light, oxygen, and voltage (LOV) sensing domain binding a flavin mononucleotide (FMN) as a chromophore noncovalently. Photoreaction of the FKF1-LOV polypeptide was studied by low-temperature absorption spectroscopy. Upon blue light irradiation, a ground state, D_{450}, is converted to S_{390} known as a cysteinyl-flavin adduct intermediate in the photoreaction of phototropin. Below 150 K, bleaching of D_{450} was much reduced and a new photoproduct, Z_{370}, appeared as well as S_{390} formation. The calculated absorption spectrum for Z_{370} is very similar to those of flavoproteins in an anion radical state. On the basis of the results that S_{390} formation proceeds to Z_{370} formation and that Z_{370} formed at low temperatures reverts to D_{450} upon temperature increase, Z_{370} is concluded to be not an intermediate from D_{450} to S_{390}. Z_{370} is suggested to be formed from the biradical triplet-excited state after relaxing to the ground state with the FMN anion radical trapped at the low temperature, in which the SH of the cysteine is in the wrong position that is able to produce a radical pair but unable to form the cysteinyl-flavin adduct. The counter SH in the cationic radical state may revert to the ground state by extracting an electron from the unidentified amino acid residue. Interestingly, S_{390} that has been thought to be irreversible to D_{450} was revealed to revert to D_{450} very slowly with a half-life time of 62.5 h in solution at 298 K. The photoreaction mechanism is discussed in reference to the calculated activation energy of the reaction processes.

Plants have acquired three major photoreceptive pigments, a red/far-red photoreversible receptor, phytochrome, and two blue light receptors, cryptochrome and phototropin (phot),[1] to sense their environmental conditions during the evolutional processes. Phot (1, 2) was first identified as a photoreceptor for tropic responses in *Arabidopsis thaliana* (*A. thaliana*) (3) and then proved to be a photoreceptor for chloroplast relocation (4, 5) and stomata opening (6). Phot has two chromophoric domains in the N-terminal half named LOV (light, oxygen, and voltage) (7–9) that bind a FMN noncovalently. The LOV domains are known to be a subfamily of the PER-ARNT-SIM (PAS) superfamily thought to act as protein–protein interaction modules in eukaryotic cellular signaling (10). Phot has isoforms phot1 and phot2, in *A. thaliana*, that show different light sensitivity and share the regulatory functions (11).

In addition to the phot families, *A. thaliana* has three more unique proteins that have only one LOV domain, named ZTL (LKP1, ADO1) (12–14), LKP2 (ADO2) (15, 16), and FKF1 (LKP3, ADO3) (17). All of them have three characteristic domains, a LOV domain, a F-box, and a Kelch repeat in this order from the N- to the C-termini. The function of the F-box is to interact with SKP proteins that are a component of the SCF (Skp/Cullin/F-box) class of E3 ubiquitin ligases that link the target substrates to the core ubiquitinating activity of the ligase complex (18, 19). Kelch repeat, while, is known to act as a protein–protein interacting site (16, 20). FKF1 has been shown to be involved in the light-regulated expression of *CONSTANS* (*CO*) (17), one of a key gene in day-length discrimination leading to flowering under long-day conditions through controlling the expression of a gene, *Flowering Locus T* (*FT*) (21–23), by enhancing degradation of CDF1, a repressor of *CO* expression (24) possibly through an ubiquitin–proteasome protein degradation pathway (25–27). The binding site between FKF1 and CDF1 is reported to be in the Kelch repeat region (24), and

* To whom correspondence should be addressed. Phone: +81-72-254-9841. Fax: +81-72-254-9841. E-mail: toxan@riast.osakafu-u.ac.jp.
‡ Osaka Prefecture University.
§ Kyoto University.
ǁ Nagoya Institute of Technology.

¹ Abbreviations: *A. thaliana, Arabidopsis thaliana*; *CO, CONSTANS*; *E. coli, Escherichia coli*; FKF, flavin-binding Kelch repeat F-box; FMN, flavin mononucleotide; *FT, Flowering Locus T*; GST, glutathione *S*-transferase; LKP, LOV Kelch protein; LOV, light, oxygen, and voltage; NMR, nuclear magnetic resonance; PAGE, polyacrylamide gel electrophoresis; PAS, PER-ARNT-SIM; phot, phototropin; phot1, phototropin 1; phot2, phototropin 2; phy3, phytochrome 3; ZTL, ZEITLUPE.